coatings

MDPI

Review

TiO_2-Based Photocatalytic Self-Cleaning Coatings for Building Materials: Surface Mechanisms, Performance Metrics, and Outdoor Durability

Yunzhang Li [1,*], Simeng Li [1], Zhenglin Han [1] and Tao Ding [2]

[1] School of Civil Engineering and Architecture, Taizhou Vocational and Technical College, Taizhou 318000, China; 13136587802@126.com (S.L.); 18005806266@163.com (Z.H.)
[2] State Key Laboratory Advanced Special Steel, Shanghai Applied Radiation Institute, Shanghai University, Shanghai 200444, China; dingtao202109@163.com
* Correspondence: liyunzhangi@126.com

Abstract

Building facades and construction materials are continuously exposed to airborne particulate matter, organic pollutants, and microbial colonization, which cause progressive soiling, aesthetic degradation, and structural deterioration while imposing high maintenance and energy burdens. Photocatalytic titanium dioxide (TiO_2) has emerged as the most widely studied material for imparting self-cleaning functionality to building surfaces, owing to its ability to mineralize adsorbed contaminants under solar irradiation and to modulate surface wettability. This narrative review provides a structured account of TiO_2-based self-cleaning coatings for building materials, organized around three complementary themes: surface mechanisms, performance metrics, and outdoor durability. We first rationalize the two intertwined self-cleaning mechanisms—photocatalytic oxidative degradation and photoinduced superhydrophilicity—and their combination with physically repellent (superhydrophobic/superamphiphobic) wetting states. We then survey the principal coating-design strategies, including morphology and facet engineering, SiO_2-TiO_2 composites, metal/non-metal doping and heterojunction construction for visible-light activation, and dual-functional photocatalytic–superhydrophobic systems, and their integration into cementitious substrates, natural stone and cultural heritage, and transparent glass/photovoltaic surfaces. The quantitative metrics used to benchmark self-cleaning performance—water contact angle, dye photodegradation, NO_x and VOC abatement, and antimicrobial activity—are critically discussed together with the limitations of standardized laboratory tests. Finally, we analyze the weathering-induced deactivation pathways (photocatalyst leaching, surface contamination by soluble salts, and UV aging of organic matrices) and the emerging strategies for durable coatings, including inorganic binders, light-driven hydration, and defect- and heterojunction-engineered photocatalysts. The review concludes with an outlook on the open challenges that must be addressed to translate these coatings from laboratory demonstrations to long-lived, large-scale building applications.

Keywords: titanium dioxide; photocatalytic self-cleaning; photoinduced superhydrophilicity; building materials; outdoor durability; visible-light photocatalysis; superhydrophobic coating

Check for updates

Academic Editor: Martina Gilić

Received: 24 August 2026
Revised: 2 September 2026
Accepted: 4 September 2026
Published: 6 September 2026

Copyright: © 2026 by the authors. Licensee MDPI, Basel, Switzerland. This article is an open access article distributed under the terms and conditions of the Creative Commons Attribution (CC BY) license.

1. Introduction

The built environment is continuously exposed to a chemically aggressive and particulate-laden atmosphere. Vehicular and industrial emissions deposit soot, polycyclic

aromatic hydrocarbons, inorganic dust, and biological species onto building envelopes, where they are progressively fixed by rain, humidity, and UV irradiation [1–3]. The resulting soiling degrades the aesthetic value of facades, reduces the solar reflectance (albedo) of "cool" surfaces and thereby their thermal benefit, and accelerates the physicochemical deterioration of porous substrates through salt crystallization, acid attack, and microbial colonization [3–6]. Conventional remediation by periodic cleaning is costly, water-intensive, and often chemically aggressive, which has motivated the development of self-cleaning surfaces that maintain their appearance with minimal intervention [7–9].

Among the candidate functional materials, titanium dioxide (TiO_2) is by far the most extensively investigated photocatalyst for construction applications [10–12]. Following the landmark recognition of its water-splitting ability and, later, the discovery of photoinduced superhydrophilicity, TiO_2 has been commercialized in self-cleaning glass, coatings, and paints. Its appeal stems from a favorable combination of high photocatalytic activity, chemical and photochemical stability, low toxicity, earth abundance, and low cost [11,13,14]. Anatase, the most photoactive polymorph, possesses a band gap of approximately 3.2 eV, which confines direct photoactivation to the ultraviolet (UV) fraction (~3%–5%) of the solar spectrum and has accordingly driven extensive efforts toward visible-light sensitization through doping and heterojunction engineering [14–18].

TiO_2-based self-cleaning is conventionally attributed to two synergistic mechanisms. Upon irradiation with photons of sufficient energy, photogenerated electron–hole pairs interact with adsorbed H_2O and O_2, generating highly reactive species such as hydroxyl radicals ($^{\bullet}OH$) and superoxide radicals ($^{\bullet}O_2^-$), while photogenerated holes (h^+) can directly oxidize surface-bound contaminants. Collectively, these oxidative species promote the degradation and eventual mineralization of adsorbed organic pollutants into CO_2 and H_2O [11,19,20]. In parallel, UV irradiation induces a superhydrophilic transition of the TiO_2 surface, reducing the water contact angle to nearly 0°. This enhanced wettability enables rainwater to spread into a continuous film, thereby facilitating the removal of loosely adhered contaminants and debris [13,21,22]. Recent studies have further complemented these mechanisms through deliberately engineered superhydrophobic or superamphiphobic surface topographies, which promote droplet rolling and particulate removal via a lotus-leaf-like effect [23–26]. Integrating photocatalytic degradation with tailored surface wettability—whether superhydrophilic or superhydrophobic—is therefore widely recognized as an effective strategy for achieving robust and durable self-cleaning performance [9,23,27].

Despite substantial advances in the field, the practical implementation of TiO_2-based self-cleaning coatings remains limited by several interrelated challenges. The interplay between photocatalytic activity and irradiation-induced changes in surface wettability is strongly influenced by coating microstructure, substrate properties, and ambient humidity; however, the contributions of these processes are often insufficiently distinguished in the literature [1,28]. Compounding this mechanistic ambiguity is a lack of standardized evaluation. Performance metrics across studies—such as contact angles, dye discoloration, NO_x conversion, and antibacterial activity—are rarely comparable due to the use of disparate model pollutants, light sources, and exposure protocols [10,29,30]. Most critically, the long-term outdoor durability of these coatings remains largely unproven. Under real-world weathering, photocatalytic efficiency typically deteriorates owing to catalyst leaching, deactivation by soluble salts, and the UV-induced degradation of organic binder matrices [1,2,4,31–33].

This review synthesizes the recent literature on TiO_2-based photocatalytic self-cleaning coatings for building materials. Rather than cataloging formulations only by composition, the discussion follows the causal sequence from surface mechanism, through coating

architecture and substrate integration, to measurement and durability. The fundamental mechanisms governing contaminant degradation and light-induced changes in surface wettability are first elucidated, followed by a critical examination of major design and fabrication strategies, including morphological control, SiO_2–TiO_2 composite architectures, visible-light-responsive modification, and dual-functional superhydrophobic systems. The compatibility and integration of these coatings with the principal classes of building materials are subsequently assessed. Particular attention is devoted to performance metrics, testing protocols, outdoor weathering, and durability under realistic service conditions. The review concludes by identifying unresolved scientific and technological challenges and outlining priorities for future research. Throughout, quantitative performance claims are interpreted in relation to their specific experimental conditions, with emphasis placed on the mechanistic uncertainties and methodological inconsistencies that continue to impede practical implementation.

2. Surface Mechanisms of TiO_2-Based Self-Cleaning

The self-cleaning action of a TiO_2-based coating arises from the interplay of three surface phenomena: (i) photocatalytic oxidative degradation, (ii) photoinduced superhydrophilicity, and (iii) engineered wetting states (hydrophobicity/superhydrophobicity) that physically remove contaminants. This section describes each mechanism and their combination.

2.1. Photocatalytic Oxidative Degradation

Figure 1 provides an author-generated synthesis of the complementary chemical and physical routes by which TiO_2 coatings clean exposed building surfaces. Figure 1a traces light absorption, charge separation, reactive oxygen species formation, and contaminant mineralization; Figure 1b links irradiation to surface hydroxylation and water-sheet formation; and Figure 1c summarizes the progression from an organic stain to photochemical fragmentation and rinsing. These mechanisms are based on the literature discussed in refs. [11,23].

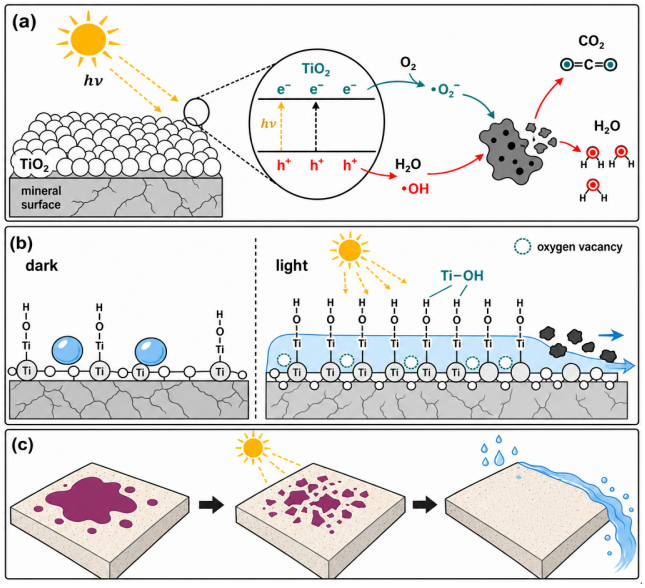


Figure 1. Original schematic summary of TiO_2-based self-cleaning mechanisms: (**a**) photon-induced charge separation and reactive oxygen species formation for oxidative mineralization; (**b**) photoinduced hydroxylation and water-sheet formation; and (**c**) conceptual stain fragmentation followed by rinsing. Drawn by the authors based on the mechanisms discussed in Refs. [11,23].

Photocatalytic degradation is the chemical cornerstone of TiO_2 self-cleaning. Upon absorption of photons with energy exceeding the band gap, electrons are promoted from the valence band to the conduction band, leaving holes in the valence band [11,19]. The elementary steps are commonly summarized as follows:

$$TiO_2 + h\nu \rightarrow e^-_{CB} + h^+_{VB} \quad (1)$$

$$h^+_{VB} + H_2O/OH^- \rightarrow {}^\bullet OH + H^+ \quad (2)$$

$$e^-_{CB} + O_2 \rightarrow {}^\bullet O_{2^-} \quad (3)$$

Provided that charge carriers migrate to the surface before recombining, holes, hydroxyl radicals, superoxide, and downstream oxygen species oxidize adsorbed organics through intermediates toward CO_2, H_2O, and inorganic ions [19,20]. Their relative contributions are not universal. Radical-scavenging experiments on TiO_2–SiO_2 hydrosol coatings identified holes and superoxide radicals, rather than hydroxyl radicals, as the dominant reactive species under the tested UV conditions, illustrating the dependence of the reaction pathway on surface chemistry, oxygen availability, humidity, and pollutant adsorption [20]. Dye disappearance alone therefore demonstrates neither complete mineralization nor a particular ROS pathway; total organic carbon, intermediate-product analysis, selective quenching, or electron-paramagnetic-resonance evidence is required for stronger mechanistic attribution.

The photocatalytic efficiency of TiO_2 is governed by several intrinsic and extrinsic factors. Crystallite size and exposed morphology exert a pronounced influence: films of 6–9 nm anatase quasi-cubic and octahedral particles degraded 80% of adsorbed methylene blue (MB), markedly outperforming larger (30–50 nm) or flower-like particles, an effect attributed to the higher specific surface area and reduced bulk recombination of nanocrystalline titania [34]. Facet engineering provides a further lever, since anatase nanosheets exposing a high fraction of high-energy {001} facets exhibit substantially enhanced photoactivity relative to conventional P25 after removal of adsorbed fluoride residues [35]. Micro- and mesoporosity likewise promote activity by increasing the accessible surface area and the density of active sites [33,36,37].

A key intrinsic limitation of pristine TiO_2 is its wide band gap (approximately 3.2 eV for anatase), which confines its photoresponse primarily to the UV region [13,14]. Elemental doping and heterojunction engineering have therefore been extensively investigated to enhance visible-light utilization, as discussed in Section 3.3. Non-metal dopants, such as nitrogen, can introduce localized electronic states within the band gap, thereby lowering the effective excitation energy and promoting photocatalytic activity under visible-light irradiation [10,38]. Incorporation of metal species—including Ag, Au, Cu, Fe, Ce, Mo, Ca, and Mg—can modify the electronic structure, create oxygen vacancies or carrier-trapping sites, and suppress electron–hole recombination; plasmonic metals such as Ag and Au may additionally enhance visible-light absorption through localized surface plasmon resonance [12,14–18,39,40]. Heterojunction architectures, including type-II, Z-scheme, and S-scheme configurations, further facilitate charge separation and interfacial carrier transfer between coupled semiconductors. In particular, Z-scheme and S-scheme systems can retain charge carriers with strong redox capabilities while simultaneously extending light absorption into the visible region [41–44].

2.2. Photoinduced Superhydrophilicity

The second pillar of TiO_2 self-cleaning is photoinduced superhydrophilicity, first recognized by Wang and co-workers and since exploited to produce “water-sheeting” surfaces. Under UV illumination, the TiO_2 surface becomes highly wettable, with water

contact angles (WCA) falling from tens of degrees to below 10° or to a fully spreading state (WCA ≈ 0°) [13,21,22]. The mechanism is generally rationalized in terms of the light-driven generation of surface oxygen vacancies at bridging-oxygen sites, accompanied by the dissociative adsorption of water and the formation of surface hydroxyl groups [45]. These hydroxylated, defect-rich surfaces possess a high surface energy that strongly favors water spreading; the process is reversible in the dark, where the hydroxylated surface slowly relaxes toward a less hydrophilic state [45,46].

Photoinduced superhydrophilicity is frequently exploited together with photocatalytic degradation. The continuous water film formed on a superhydrophilic coating solubilizes water-soluble contaminants and assists the removal of particulates and oxidation residues [9,22]. Sol–gel TiO_2–SiO_2 composite coatings exemplify this cooperation: a droplet spread completely on the coating surface in 0.35 s (WCA 0°), and organic dyes on the same surface were degraded under illumination [22]. In defect-engineered Ca- and Mg-incorporated TiO_2, photoinduced hydrophilicity was quantified by the UV-induced reduction in WCA, with Ca incorporation producing the strongest effect and the greatest calculated tendency to form oxygen vacancies [16]. These measurements should report droplet volume, illumination history, delay between irradiation and measurement, relative humidity, and dark-recovery time because each can change the apparent contact angle.

It should be emphasized that superhydrophilicity is not synonymous with photocatalytic activity. A coating may be highly wettable yet weakly photoactive, and vice versa; the two properties are governed by partially distinct surface states and therefore require independent optimization [28,29]. Moreover, relative humidity modulates both the hydroxylation of the clean TiO_2 surface and, consequently, the onset and extent of superhydrophilicity, a dependence that is frequently overlooked in accelerated laboratory testing [28].

2.3. Heterojunction Charge Separation and Surface Redox

Heterojunctions alter self-cleaning at the surface by controlling where photogenerated carriers are retained, recombine, and react with adsorbed oxygen or water. Conventional type-II transfer can improve spatial separation but may weaken the reduction and oxidation potentials available for surface chemistry. Direct Z-scheme, mediator-assisted Z-scheme, and S-scheme architectures are instead designed to remove low-energy carriers while preserving strongly reducing electrons and strongly oxidizing holes. The proposed pathway must be supported by band positions together with carrier-lifetime, radical, interfacial-potential, or operando evidence; band alignment alone is not sufficient.

Figure 2 reframes the reported TiO_2 heterojunction mechanisms as an author-generated comparison rather than as reproduced source diagrams. Type-II transfer spatially separates carriers but can reduce their redox strength, whereas direct and mediator-assisted Z-schemes selectively remove weaker carriers and retain strongly reducing electrons and strongly oxidizing holes. The S-scheme additionally emphasizes band bending and the interfacial electric field. These interpretations are discussed in Refs. [18,43,44].

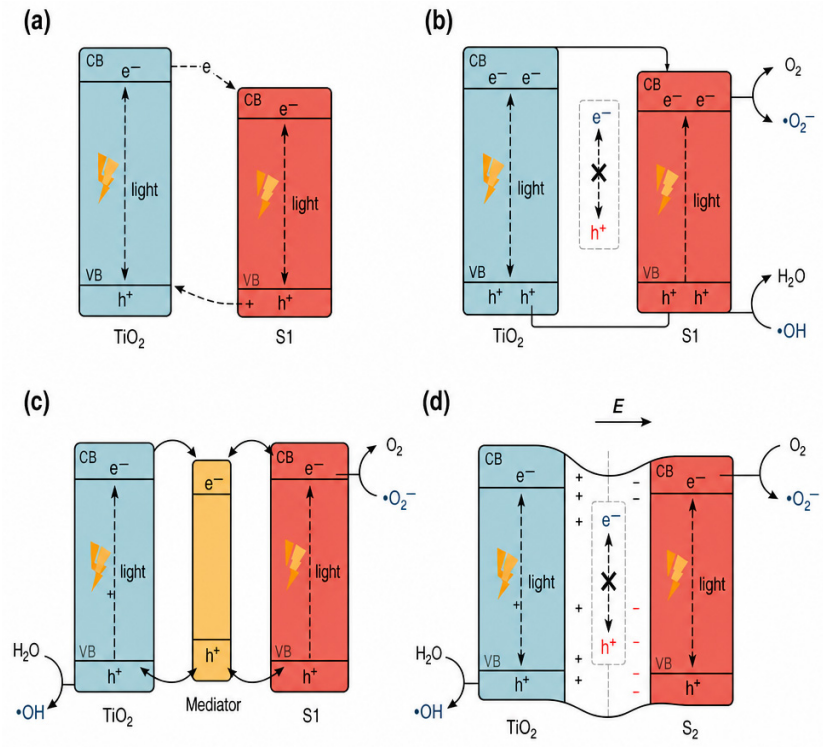


Figure 2. Original comparison of charge-transfer pathways used to interpret visible-light-active TiO_2 heterojunctions: (**a**) conventional type-II transfer; (**b**) direct Z-scheme transfer; (**c**) mediator-assisted ternary Z-scheme transfer; and (**d**) S-scheme transfer with interfacial band bending and a built-in electric field. The outer-band reactions indicate the redox capacity retained by each pathway. Drawn by the authors based on Refs. [18,43,44].

2.4. Physical Self-Cleaning: Superhydrophobic and Amphi-Repellent States

An alternative, physically driven mode of self-cleaning is conferred by superhydrophobic and superamphiphobic surfaces, which reduce liquid retention and particulate adhesion. Inspired by the lotus leaf, these surfaces combine micro/nano-scale hierarchical roughness with low-surface-energy chemistry so that water droplets exhibit a high static contact angle (>150°) and low sliding angle (<10°), allowing mobile droplets to collect loose debris [23,24,26,47]. For a chemically homogeneous smooth surface, Young's equation relates the equilibrium angle to interfacial tensions, whereas rough coatings are more appropriately interpreted through Wenzel and Cassie–Baxter descriptions:

$$\cos\theta_Y = (\gamma_{SV} - \gamma_{SL})/\gamma_{LV} \quad (4)$$

$$\cos\theta_W = r\cos\theta_Y \quad (5)$$

$$\cos\theta_{CB} = f_s(\cos\theta_Y + 1) - 1 \quad (6)$$

Here, θ_Y, θ_W, θ_{CB} denote the Young, Wenzel, and Cassie–Baxter contact angles, respectively; γ_{SV}, γ_{SL}, γ_{LV} are the solid–vapor, solid–liquid, and liquid–vapor interfacial tensions; r is the roughness ratio; and f_s is the liquid-contacting solid fraction. These idealized models are useful design guides, but sliding angle and contact-angle hysteresis are more informative than static WCA for practical soil removal because a nominally high WCA can coexist with strong pinning. When TiO_2 is embedded in or co-deposited with a hydrophobic matrix, rolling water can remove loose particulate matter, while photocatalysis attacks residual organics [23,25]. The combination is intrinsically tensioned, however: UV-generated hydroxylation can lower hydrophobicity, ROS can oxidize silanes or polymers, and excessive burial of TiO_2 by the low-energy phase reduces accessible photoactive area.

Figure 3 links coating architecture to wetting and contaminant removal without reproducing source-paper micrographs or contact-angle photographs. Figure 3a shows the development of multiscale roughness and surface functionalization, Figure 3b compares conceptual liquid states on the hierarchical coating and bare glass, and Figure 3c integrates droplet roll-off with photocatalytic oxidation. The synthesis is based on design principles reported in Refs. [26,47].

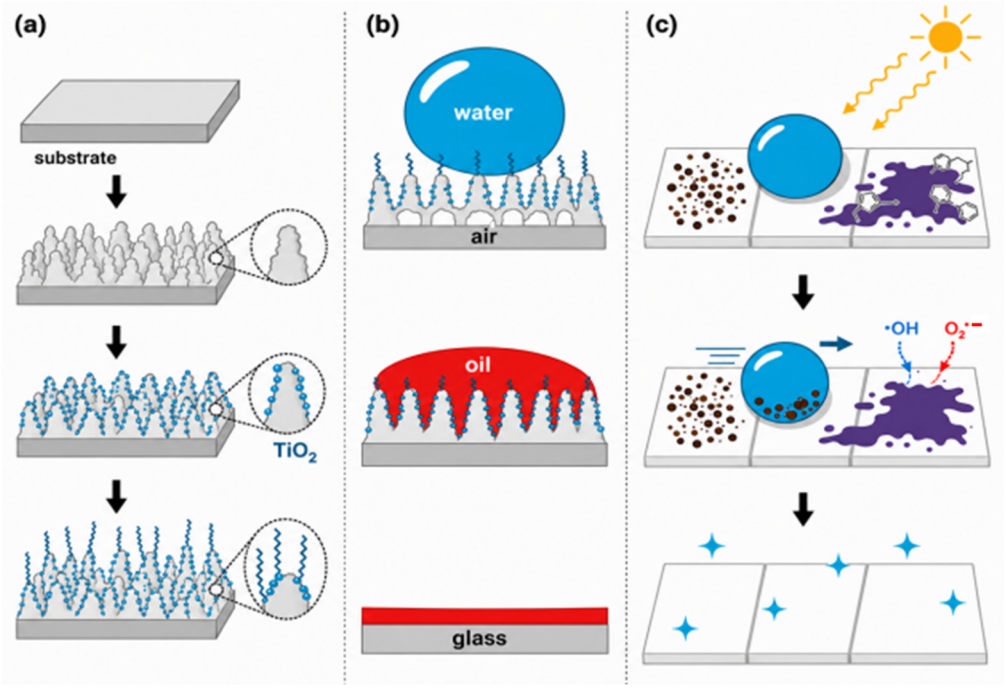


Figure 3. Original schematic linking hierarchical coating architecture to wetting and self-cleaning behavior: (**a**) evolution from a smooth substrate to a TiO_2-decorated micro-/nanostructure with low-surface-energy groups; (**b**) conceptual wetting states for water, a lower-surface-tension liquid, and bare glass; and (**c**) coupling of droplet roll-off with photocatalytic oxidation. Drawn by the authors based on Refs. [26,47].

Recent studies have quantified the benefits of this dual physical–chemical strategy. Coatings based on recycled concrete powder-supported TiO_2 in a polydimethylsiloxane (PDMS) matrix achieved WCA > 150° with sliding angles < 10°, and the coupling of superhydrophobicity with photocatalytic degradation produced self-cleaning capacities superior to either mechanism alone [23]. Fluorine-free photocatalytic–superhydrophobic coatings, in which stearic acid lowered the surface energy of dual-scale TiO_2 particles, reached WCA of 163.6° and sliding angles of 2.5° while retaining methylene blue and methyl orange photodegradation [25]. Superamphiphobic TiO_2–SiO_2/PFDTS coatings repelled water, ethylene glycol, glycerol, and hexadecane (contact angles of 163.5°, 154.6°, 157.3°, and 150.2°, respectively) while degrading 80.9% of a methyl orange solution under UV irradiation within 60 min [26].

A conceptually distinct approach combines liquid amphi-repellency (physical self-cleaning) with photocatalytic activity (chemical self-cleaning) on a smooth, transparent glass surface, using a fluorosilane and a low loading of TiO_2 nanoparticles. The selected coating (0.25 wt.% TiO_2) preserved optical transparency while exhibiting both stain resistance and photocatalytic cleaning, illustrating that repellency and photocatalysis need not require rough, light-scattering topographies [27].

2.5. Coupling Mechanisms and Design Rationale

The relative contribution of degradation, water-sheeting, and roll-off depends on the service environment and contaminant type. Water-sheeting surfaces are well suited to inclined glazing and photovoltaic modules where uniform wetting, low haze, and optical transmission are paramount [8,38,48,49]. Repellent surfaces can be advantageous where wind-borne particles, liquid water ingress, or hydrophobic soiling dominate and where substrate protection is required [4,24,50]. Neither wetting state is categorically superior. A superhydrophilic facade may retain water long enough to exacerbate salt transport on a porous stone, whereas a superhydrophobic surface may lose its Cassie state under abrasion, surfactants, or prolonged condensation. The design objective is therefore a service-specific balance among photocatalytic turnover, water mobility, optical or aesthetic compatibility, adhesion, and retention of function after weathering [9,27].

The coupling is therefore sequential rather than automatically additive: the coating must first expose TiO_2 and permit light and reactant transport; photogenerated carriers must then reach the interface before recombination; reactive species must contact the contaminant; and the wetting state must mobilize the remaining debris without masking or prematurely removing the catalyst. A formulation that maximizes one step can reduce another, so performance should be reported as a balance among accessible photoactivity, water mobility, adhesion, optical compatibility, and retention after weathering.

HDTMS (hexadecyltrimethoxysilane) is used in several repellent formulations as a low-surface-energy modifier; its contribution should be distinguished from the photocatalytic role of TiO_2 and evaluated for UV and oxidative stability.

3. Design and Fabrication of TiO_2-Based Coatings

The performance of a TiO_2 self-cleaning coating is largely predetermined by its composition, morphology, and the method by which it is applied. This section reviews the principal design strategies, progressing from pristine TiO_2 and morphology control, through SiO_2–TiO_2 composites, to visible-light activation and dual-functional superhydrophobic systems, and finally to carbon-based and encapsulated hybrids.

3.1. Pristine TiO_2, Morphology, and Facet Control

The photoactivity of unmodified TiO_2 is strongly dependent on particle size, morphology, porosity, and crystal phase. Nanocrystalline anatase with a high specific surface area and short carrier-diffusion lengths is generally most active, as demonstrated by the superior MB degradation of 6–9 nm quasi-cubic/octahedral particles relative to larger or flower-shaped counterparts [34]. Controlled hierarchical porosity is likewise beneficial: porous TiO_2 microspheres blended into cement outperformed P25/cement composites because the micro/nano hierarchical structure enhanced light harvesting and exposed more reactive sites [36]. Similarly, reticulated mesoporous TiO_2 layers achieved 100% self-cleaning efficiency for both thick and thin films after low-temperature annealing, with visible transmittance of roughly 60%–80% [37].

Facet engineering represents a more sophisticated route. Anatase nanosheets exposing a high proportion of reactive facets, once freed of adsorbed fluoride by NaOH washing, dispersed readily and delivered dramatic improvements in the degradation of NO_x, soot, and organic dyes under simulated sunlight [35]. Morphology also dictates the optical and wetting balance required for transparent applications, since porosity and roughness that enhance photoactivity may simultaneously increase light scattering and haze [51,52]. A sustainable, low-cost alternative is the high-energy ball milling of natural TiO_2 minerals (rutile and leucoxene), which reduces crystallite size and increases surface area and UV-induced hydrophilicity; although the resulting photocatalytic activity is modest (12.8%

Rhodamine B degradation for rutile after 8 h), it is attractive where eco-friendliness and cost are prioritized over peak performance [53].

3.2. SiO_2–TiO_2 Composite Coatings

Silica is the most widely used companion oxide to TiO_2, serving multiple functions: it suppresses TiO_2 nanoparticle agglomeration, increases mechanical robustness and adhesion to mineral and glass substrates, reduces the effective refractive index (favoring antireflective behavior), and contributes intrinsic hydrophilicity [5,20–22,48,51,52,54]. The SiO_2–TiO_2 system is consequently the workhorse of transparent and superhydrophilic self-cleaning coatings.

In the antireflective domain, raspberry-like hollow SiO_2@TiO_2 nanospheres achieved a refractive index of 1.218 and transmittance above 99% while retaining excellent photocatalytic self-cleaning [51]. Robust SiO_2@TiO_2 nanocoatings incorporating commercial P25 were prepared by simple dip-coating, balancing antireflection and photocatalytic activity without post-treatment [52]. On glass, SiO_2–TiO_2 nanostructured coatings delivered superhydrophilicity (WCA 11.3°) together with a >16% enhancement in optical transmittance and substantial reductions in soiling density, improving photovoltaic efficiency under tilt [48]. For building stone and concrete, SiO_2–TiO_2 composites simultaneously consolidate friable substrates and impart self-cleaning: a TiO_2–SiO_2 nanocomposite formed within the pores of a friable carbonate stone by simple spraying converted the stone into a self-cleaning building material and protected it against salt crystallization for over 30 cycles, far exceeding the untreated stone, which powdered after only three cycles [5].

The preparation route strongly influences the resulting interface. TiO_2–SiO_2 composite hydrosols synthesized from a peroxo titanium precursor via Fe_3O_4-catalyzed Fenton-like reaction yielded anatase nanorods with BET surface areas exceeding 200 $m^2\ g^{-1}$, achieving 72% MB degradation within 5 min under UV light and complete discoloration within 30 min, with holes and superoxide radicals identified as the dominant reactive species [20]. Coatings derived from such hydrosols sustained photocatalytic performance through 17 pull-off cycles and 6 h of water impact, illustrating the adhesion conferred by a cohesive silica network [20]. Similarly, sol–gel TiO_2–SiO_2 coatings on Carrara marble produced a fully spreading (WCA $\approx 0°$) surface that degraded 74.35% of MB within 12 h under UV and maintained superhydrophilicity through 20 tape-peeling cycles [21]. Rod-like TiO_2–SiO_2 core–shell nanoparticles applied by dip-coating further extended SiO_2–TiO_2 coatings to the visible-light-driven removal of organic pollutants, imparting a ~4% optical-transmission enhancement on glass together with good mechanical stability [55].

3.3. Visible-Light Activation by Doping and Heterojunction Materials

This subsection focuses on material-design routes that implement visible-light activation after the charge-transfer mechanisms in Section 2.3 have been established. Doping changes the electronic structure of TiO_2, whereas heterojunction construction combines complementary absorbers and interfaces; in both cases, the reported performance must be interpreted together with coating accessibility, substrate compatibility, and durability.

Nitrogen doping is the most established route, introducing states above the valence band that narrow the effective band gap. N-doped TiO_2 coatings on travertine stone exhibited visible-light photocatalytic activity comparable to or better than P25, with the dopant-introduction route (acidic process versus urea) influencing activity and highlighting the dependence of self-cleaning evaluation on the choice of model dye [10]. A SiO_2/N-TiO_2 heterostructure for a solar-module glass cover combined a porous antireflective SiO_2 underlayer with an N-TiO_2 overlayer, achieving higher optical transmittance than pristine

TiO_2 and a minimum WCA of 11.9°, with density-functional-theory (DFT) calculations rationalizing the visible-light response [38].

Metal dopants act through band-gap modification, charge trapping, and the introduction of oxygen vacancies. Copper and iron doping of TiO_2 thin films narrowed the measured optical band gap from ~3.20 eV (pure) to ~2.65 eV (Fe) and ~2.40 eV (Cu), with 0.8% Cu- and 3% Fe-doped films exhibiting the best hydrophilicity and MB degradation, respectively, under the reported conditions [14]. Cerium doping produced anatase/brookite nanoparticles (~10 nm) that degraded 97.08% of MB under visible light in 240 min, with reduced photoluminescence consistent with suppressed recombination [17]. Molybdenum-doped TiO_2–LDH suspensions applied to brick and stone provided visible-light self-cleaning, with an optimum Mo/Ti mass ratio of 0.03 [15]. Noble-metal modification is also effective: Au–TiO_2 integrated into a silica sol–gel showed that the smallest Au nanoparticles (13 nm) and an intermediate loading (0.5 wt.% Au/TiO_2) maximized soot and NO abatement [12], while Ag–SiO_2–TiO_2 coatings with 10 wt.% Ag enhanced photoactivity through visible-light absorption and increased surface area [39]. Defect engineering with earth-abundant cations is an emerging alternative: Ca- and Mg-incorporated anatase nanopowders (particle size ~12.5–13.5 nm, surface area ~235 $m^2\ g^{-1}$) delivered ~97% Rhodamine B degradation under simulated solar light, with DFT supporting an oxygen-vacancy-driven mechanism in which calcium promotes vacancy formation most effectively [16]. Apparent band-gap narrowing alone should not be taken as proof of useful visible-light photocatalysis because dopant-induced states can also act as recombination centers; wavelength-resolved action spectra and stable multi-cycle activity provide stronger evidence.

The construction of heterojunctions between TiO_2 and a second semiconductor can extend absorption and alter charge-carrier separation. p-BiOI/n-TiO_2 heterojunctions imparted visible-light self-cleaning to cotton fabrics [41], and BiOI/TiO_2 heterostructures immobilized on glass, interpreted as an S-scheme configuration, outperformed pure TiO_2 and BiOI in self-cleaning tests under simulated solar light [44]. A VO_2@Fe_2O_3–TiO_2 nanocomposite reduced the measured band gap from 2.86 to 2.00 eV and achieved 88.81% MB degradation in 120 min under visible light, compared with 15.84% for Fe_2O_3–TiO_2, and was interpreted through a Z-scheme pathway [18]. A Co^{2+}-TiO_2/$LaNiO_3$ direct Z-scheme heterojunction combined carrier separation and micropatterning to enhance superhydrophilicity and photocatalytic activity [43]. In a similar vein, 2D g-C_3N_4/1D TiO_2-nanorod heterojunctions dispersed in a PVDF/PTFE matrix endowed coatings with visible-light photocatalysis and superhydrophobicity [42]. Because type-II, Z-scheme, and S-scheme labels are sometimes assigned from band-edge diagrams alone, robust mechanism claims should combine band-position measurements with carrier-lifetime, radical, interfacial-potential, or in situ spectroscopic evidence.

3.4. Dual-Functional Photocatalytic–Superhydrophobic Coatings

The deliberate co-design of photocatalysis with superhydrophobicity has become one of the most active research directions, motivated by the complementary roles of the two mechanisms. A common strategy is to embed TiO_2 (often surface-modified with a hydrophobic silane) into a low-surface-energy polymer matrix. Representative systems and their key figures of merit are summarized in Table 1.

Table 1. Representative dual-functional photocatalytic self-cleaning coating systems and their key performance metrics.

Coating System	Wettability	Photocatalytic Performance	Durability/Notable Feature	Ref.
A-SiO_2/N-TiO_2@HDTMS	WCA 157.2°; SA 2.7°	Methyl orange degradation	Self-healing (8 h dark storage); 3 months outdoor	[46]
FEP/TiO_2–SiO_2 (electrostatic spray)	WCA > 150°	Oleic acid and MB degradation	Stable at pH 5–11	[56]
RCP@TiO_2/PDMS	WCA > 150°; SA < 10°	Photocatalytic degradation	Stain resistance; abrasion and water-impact stability	[23]
TiO_2–SiO_2/PFDTS	WCA 163.5° (superamphiphobic); SA 0.4°	80.9% methyl orange in 60 min (UV)	Broad substrate and liquid adaptability	[26]
Sericite-TiO_2/HDTMS	WCA 154.7°; SA 2.1°	35.8% methyl orange in 50 min (UV)	UV-aging resistance (WCA ≈ 150° after 40 h)	[47]
PDMS/EP/STA/TiO_2 (fluorine-free)	WCA 163.6°; SA 2.5°	MB and methyl orange degradation (UV)	64 tape peels; 55 sandpaper frictions; 6 months outdoor	[25]
Sodium laurate/nano-TiO_2 (concrete)	WCA 159.8°; SA 5.1°	99.1% NO degradation	Stable after UV aging and thermal cycling	[24]
Doped TiO_2/oligomethylhydrosiloxane	WCA 140–145°	99.9% rhodamine 6G (visible)	Water absorption 4%–15% after 1 h immersion	[57]
h-BN/TiO_2-WO^{3+} fluorinated TiO_2/SiO_2	WCA 151°; superamphiphobic	Photocatalytic activity	500 h salt-spray resistance	[58]

Fluorine-free formulations have attracted particular attention owing to environmental concerns over perfluorinated compounds. A one-step sprayed PDMS/epoxy/stearic-acid/TiO_2 coating reached WCA 163.6° and sliding angle 2.5°, endured 64 tape-peelings and 55 sandpaper frictions, withstood 18 h of UV exposure, and remained superhydrophobic for up to 6 months outdoors [25]. A sodium-laurate-modified nano-TiO_2 coating on concrete achieved WCA 159.8°, sliding angle 5.1°, and 99.1% NO degradation, retaining contact angles above 157° after UV aging and thermal cycling [24]. Self-healing superhydrophobic behavior has also been reported: an A-SiO_2/N-TiO_2@HDTMS coating whose UV-induced wettability transition spontaneously recovered to superhydrophobicity after 8 h of dark storage, and which maintained self-cleaning after 3 months outdoors [46]. Large-scale, one-step fabrication routes are exemplified by electrostatic spraying of a fluorinated-ethylene-propylene/nano-SiO_2/TiO_2 composite, which yielded a superhydrophobic photocatalyst (WCA > 150°) with stable photocatalytic activity in acidic and alkaline media [56]. Aqueous-emulsion oligomethylhydrosiloxane formulations loaded with doped TiO_2 likewise imparted simultaneous superhydrophobicity (WCA 140–145°) and visible-light photocatalysis (99.9% rhodamine 6G degradation) to wood, brick, and aerated-concrete substrates while reducing their water absorption from ~56%–60% to 4%–15% [57].

Inorganic UV-shielding carriers address the vulnerability of organic hydrophobic modifiers to photodegradation. Sericite-supported TiO_2, modified with hexadecyltrimethoxysilane, delivered WCA 154.7° and sliding angle 2.1°, while retaining near-superhydrophobic behavior (WCA ≈ 150°) even after 40 h of UV irradiation, thanks to the UV-screening role

of the sericite carrier [47]. Hierarchical inorganic–organic systems have been extended to multifunctional architectures combining self-cleaning with corrosion resistance: an h-BN/TiO_2-WO_3 ceramic underlayer produced by micro-arc oxidation, overcoated with a fluorinated TiO_2/SiO_2 superamphiphobic layer, maintained hydrophobicity after 500 h of salt-spray exposure [58]; and a BiVO4/TiO_2 hot-dip zinc coating exhibited hydrophobicity, corrosion inhibition (91.68%), and stability after 21 days in NaCl solution [59].

3.5. Carbon-Based and Encapsulated Hybrid Systems

Carbon nanomaterials, particularly graphene oxide (GO), enhance TiO_2 photoactivity by acting as electron acceptors that suppress charge recombination and by extending the light-absorption range through Ti–O–C bonding [11]. The incorporation of up to 1 wt.% GO into TiO_2 films improved MB degradation and transmittance, although excess GO offered no further benefit [34]. A comprehensive review of TiO_2/GO composites highlights their exceptional superhydrophilicity and visible-light self-cleaning, with applications extending from glass to solar cells, paints, and building materials [11]. Carbon nanotubes, carbon black, and graphene-family materials have additionally been explored as multifunctional (self-cleaning, self-sensing, self-heating) additives for civil-construction materials, though dispersion and environmental-leaching concerns remain [60].

Microencapsulation integrates self-cleaning with self-repairing functionality for decorative coatings. $CaCO_3$/TiO_2 hybrid microcapsules with a linseed-oil core degraded methylene blue and healed micro-cracks, with an optimum loading of 7.0 wt.% and coatings retaining 3H hardness [61]. Analogous TiO_2/SiO_2-hybrid-wall microcapsules achieved a 44.4% MB degradation rate, 58.7% micro-crack self-repair, and a contact angle of 91.2° at 20% loading [62].

3.6. Deposition Route and Coating Architecture

Composition cannot be separated from processing because the deposition route controls film thickness, pore connectivity, optical scattering, catalyst exposure, and interfacial adhesion. Sol–gel dip-coating provides fine control on oxide chemistry and is particularly suitable for flat glass, but repeated withdrawal and thermal consolidation can be difficult to translate to large or porous facades. Spray application is more compatible with irregular stone, concrete, and field repair and is used in several of the building-focused studies [5,12,13,29,30,35,40]. Its practical advantages are offset by spatial variation in deposited mass, overspray, penetration into pores, and sensitivity to nozzle, distance, and rheology. Brush and roll application are simple, but can produce thicker, less uniform films; in the long-term PV study, spraying outlasted brushing, showing that application route remained important even at identical nominal chemistry [8].

In situ growth, hydrothermal processing, electrospinning, and micropatterning can create highly exposed or mechanically interlocked architectures [43,47,48]. These routes are valuable for controlled substrates but generally demand higher temperature, longer processing, specialized equipment, or substrate geometries that constrain facade-scale use. For cementitious materials, applying TiO_2 before complete setting can deliberately couple the coating to ongoing hydration and improve the interface [45]. Conversely, simply mixing TiO_2 into bulk cement protects particles mechanically but buries a large fraction away from light and reactants; surface-localized coating can therefore achieve similar activity with much lower catalyst consumption [63,64].

Figure 4 consolidates the shared design logic of dual-functional photocatalytic–water-repellent systems into a new author-generated schematic. The cross section separates substrate adhesion, accessible TiO_2, hierarchical roughness, and low-surface-energy functionality; the remaining panels distinguish droplet-mediated particle removal, photocat-

alytic oxidation of adhered organics, and conceptual recovery after surface damage. The design concepts are discussed in Refs. [25,46].

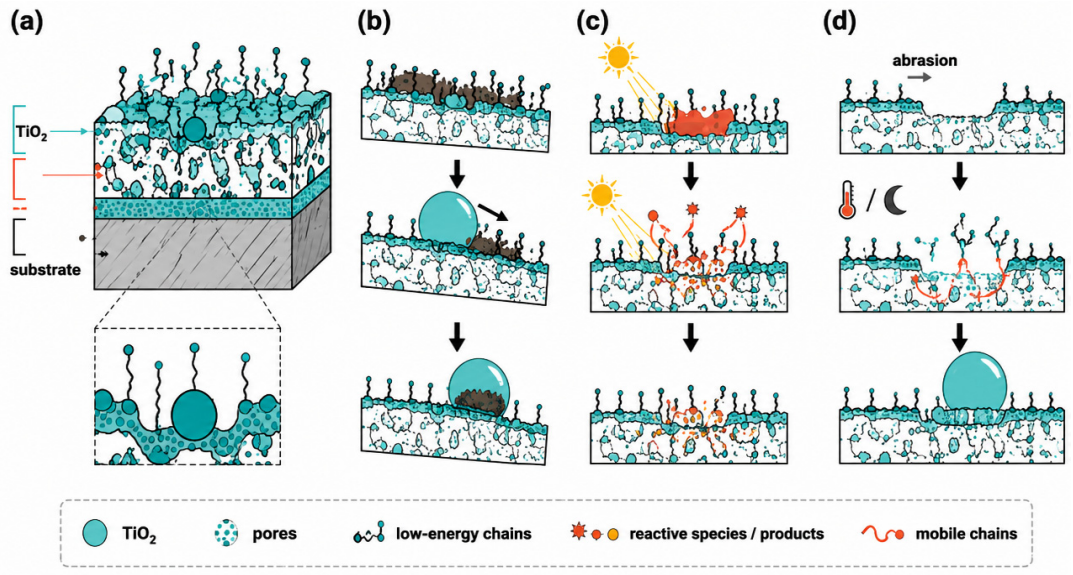


Figure 4. Original schematic of a multifunctional, hierarchically structured TiO_2 coating: (**a**) through-thickness architecture; (**b**) physical removal of particulate matter by droplet roll-off; (**c**) photocatalytic oxidation of an adhered organic contaminant; and (**d**) conceptual recovery of low-surface-energy functionality after abrasion while TiO_2 remains accessible. Drawn by the authors based on design concepts in refs. [25,46].

The practical design variable is not merely thickness but the through-thickness distribution of functions. A useful architecture may comprise a substrate-compatible primer or consolidant, a mechanically coherent TiO_2-rich active layer, and, where needed, an optically thin or discontinuous low-energy surface treatment. Continuous organic encapsulation can improve adhesion and water resistance but shield TiO_2; excessive exposed TiO_2 can instead accelerate binder oxidation. Reporting should therefore include deposited mass per area, dry thickness and variability, number of passes, curing temperature and humidity, surface roughness, adhesion, and the fraction of TiO_2 accessible at the outer surface. These process descriptors are often more transferable to scale-up than precursor molar ratios alone.

4. Application to Building Materials

The translation of TiO_2 coatings to practice depends critically on their compatibility with the substrate, which governs adhesion, durability, and the preservation of the substrate's appearance and function.

4.1. Cementitious Materials: Concrete, Mortar, and Geopolymers

Cement-based materials are the largest-volume building substrate and have been the focus of extensive photocatalytic functionalization. TiO_2 can be introduced either as an admixture within the matrix or, more efficiently, as a surface coating [63–65]. A comparative study showed that a silicate coating containing 15% TiO_2 (by mass of solid silicate) delivered photocatalytic performance comparable to a mortar containing 2% TiO_2 by mass of cement, while requiring twenty-fold less photocatalyst [63]. The physical form of TiO_2 is decisive: because powder TiO_2 agglomerates and re-disperses poorly, hydrosol-based nano-TiO_2 dispersions are preferred, and a low-dosage anatase hydrosol outperformed commercial P25 powder for Rhodamine B discoloration and NO_x conversion on Portland cement paste [64]. Colored (pigmented) mortars retain self-cleaning and photocatalytic activity

upon TiO_2 incorporation, extending the approach to aesthetic cementitious finishes [66], and cementitious coatings have also been produced from industrial residues, as in the case of TiO_2-coating cement materials prepared by the solidification/stabilization of electrolytic manganese residue, coupling waste valorization with self-cleaning functionality [67].

Metal-doping extends the depolluting scope of cementitious coatings. Cu-TiO_2/SiO_2 photocatalysts sprayed on concrete achieved 95% methylene blue and 50% soot removal (at 5% Cu loading), with activity declining at higher loadings [40]. Au-TiO_2/SiO_2 coatings similarly promoted soot and NO removal on building substrates [12]. The durability of these coatings on concrete has been explicitly assessed: TiO_2/SiO_2-coated concrete retained practically unchanged photocatalytic efficacy after four months of real outdoor exposure and three MB degradation cycles [33].

Beyond conventional cement, geopolymers and alkali-activated materials have emerged as sustainable hosts. SiO_2-supported TiO_2 on a fly-ash/slag geopolymer achieved 79.65% Rhodamine B degradation (84 h) and 74.98% NO_x removal (60 min), and—notably—retained 79.35% RhB degradation after combined UV aging and rain scouring, 2.8-fold higher than pure nano-TiO_2, while increasing 28-day compressive strength by 8.76 MPa [68]. A ceramic waste-slag geopolymer with a nano-SiO_2-TiO_2 coating reached a WCA of 118° and exhibited photocatalytic degradation of methyl orange, oleic acid, and bauxite residue [69]. Polymeric carbon nitride-functionalized alkali-activated slag composites combined NO_x removal with self-cleaning, though the photocatalyst modified hydration and microstructure [70]. Fly-ash geopolymer membranes with TiO_2 achieved up to 99.3% MB removal with UV-assisted regeneration [71].

Functionalized cementitious composites illustrate the breadth of achievable multifunctionality. Ultra-high-toughness cementitious composites incorporating C,N-co-modified TiO_2 gained simultaneous mechanical reinforcement (via enhanced hydration and densification) and photocatalytic activity [72]. Permeable (pervious) concrete with nano-TiO_2 hydrosol showed 73.6% MB degradation after 24 h UV, with 0.4% TiO_2 recommended as the optimum content [65]. Recycled-powder-supported TiO_2 (recycled concrete powder or recycled brick powder) couples waste valorization with self-cleaning, the micro/nano roughness of the support enhancing both hydrophobicity/hydrophilicity and photocatalysis [23,73,74].

4.2. Natural Stone and Cultural Heritage

Natural stone facades and built heritage present a distinct set of requirements: coatings must be compatible with porous, heterogeneous, and often friable substrates, and must not alter the substrate color or permeability [4,5,10,13,29,30,50,75]. Photocatalytic TiO_2 coatings on limestone have been shown to preserve surface color and provide self-cleaning and depolluting functions, although the efficiency of NO_x abatement depends on substrate porosity and roughness, and the coating morphology is influenced by the choice of aqueous versus alcoholic sol [6].

Heritage-specific formulations frequently combine TiO_2 with consolidants or protective polymers. A TiO_2–SiO_2 nanocomposite formed within the pores of a friable carbonate stone by spraying simultaneously consolidated the stone and imparted self-cleaning, converting a substrate that powdered after three salt-crystallization cycles into one stable over 30 cycles [5]. For twentieth-century heritage cement, inorganic treatments combining nano-TiO_2 with ethyl silicate (TEOS) slowed carbonation and chloride diffusion while boosting soiling removal and antimicrobial activity; the study also demonstrated the inadequacy of standard tests for heterogeneous substrates and the need for realistic soiling/rain protocols [30]. TiO_2-TEOS treatments for heritage cementitious materials were likewise evaluated with a customized procedure combining artificial soiling and rain cycles, revealing

differences in photocatalytic activity as a function of substrate finish [29]. Ag-TiO_2/PDMS nanocomposites applied to Lecce stone delivered water-repellency, self-cleaning, and antimicrobial protection at low silver doping ($\leq$1 mol%), with durability confirmed through aging cycles [76].

Sustainable and biodegradable matrices are an emerging theme. A polyhydroxyalkanoate (PHA)/TiO_2 nanocomposite protected marble, basalt, and travertine without notable color change and improved hydrophobicity, although the benefit partially decayed after UV aging—an instructive illustration of the trade-off between short-term performance and long-term stability in biopolymer-based coatings [75]. Microwave-synthesized anatase TiO_2 (band gap 3.24 eV, surface area 199 m^2 g^{-1}) spray-coated on limestone produced near-zero contact angles even without UV exposure and stable photocatalytic performance over multiple cycles, offering an energy-efficient synthesis route for stone facades [13].

4.3. Glass, Photovoltaic, and Transparent Substrates

Transparent self-cleaning coatings must reconcile high photoactivity with optical clarity and, for photovoltaic (PV) applications, antireflective behavior. SiO_2–TiO_2 systems dominate this sector because silica lowers the refractive index and improves adhesion [48,51,52]. For PV modules, self-cleaning is motivated by the severe power losses caused by dust deposition, particularly in arid regions: mesoporous TiO_2/SiO_2 and ZnO/SiO_2 coatings minimized dust accumulation and boosted power output over a 30-day summer field test, with TiO_2/SiO_2 showing the most stable soiling ratio [49]. A TiO_2–SiO_2-PAA (polyacrylic acid) superhydrophilic coating was studied outdoors for one to four years, sustaining an average relative self-cleaning efficacy of ~4% on glass for three years and increasing PV power generation by 2.8% [8]. Reviews of antireflective self-cleaning technology for PV panels emphasize the reduction in cleaning frequency and water consumption as primary industrial drivers [7].

Visible-light activation is especially desirable for glazing, where UV exposure is limited indoors and the coating must remain transparent. Cu- and Fe-doped TiO_2 thin films on glass achieved band gaps of 2.40 and 2.65 eV, respectively, with superior hydrophilicity (WCA 9.8° for 0.8% Cu) and MB degradation under visible light [14]. A SiO_2/N-TiO_2 heterostructure delivered high transmittance with a minimum WCA of 11.9° [38], and BiOI/TiO_2 heterostructures provided visible-light self-cleaning on glass [44]. On polymer substrates, TiO_2/SiO_2 coatings on polycarbonate preserved >85% transmittance with superhydrophilic wetting [54], and TiO_2 coatings on lightweight polycarbonate were shown to impart photocatalytic and nanomechanical function [77]. Fluorocarbon/TiO_2-SiO_2 transparent coatings combined WCA 4.5°, 96% methyl orange decolorization, and high UV stability for outdoor use [78]. Transparent hydrophobic SiO_2/TiO_2 coatings on solar-cell cover glass maintained water contact angles of 121.7–143.2° while repelling dust, with self-cleaning confirmed on a photovoltaic module [79]. Polyurethane coatings integrating an Ag_3PO_4/TiO_2 nanocomposite over a silica buffer layer achieved 58% MB degradation within 3 h under visible light, together with 86% transmittance and anti-fogging behavior [80]. Beyond TiO_2, hollow MgF_2 nanoparticles have been explored as low-refractive-index additives to enhance the transmittance of self-cleaning TiO_2 coatings [81].

4.4. Other Substrates: Wood, Textiles, Painted Surfaces, and Metals

The versatility of TiO_2 coatings extends to secondary building substrates. Photocatalytic self-cleaning coatings were applied directly to painted surfaces without an interlayer by dispersing TiO_2 in a hybrid organosilane binder; coatings with 33%–45% TiO_2 exhibited self-cleaning while protecting the underlying latex film from UV damage [82]. Eco-friendly interior paints incorporating N-doped porous TiO_2 removed p-xylene and disinfected E.

coli under indoor illumination [83]. Ag-doped TiO_2 coatings on wood provided 90% MB photodegradation under UV and suppressed bacterial colonization [84], and modified TiO_2 nanoparticles imparted dynamic hydrophobicity to traffic-marking coatings [85]. On metals, hot-dip zinc coatings modified with $BiVO_4/TiO_2$ combined hydrophobicity with corrosion resistance [59], while radiative-cooling glass-fiber textiles hybridized with TiO_2 combined solar reflectance, superhydrophobicity, and photocatalytic cleaning [86].

Photocatalytic membranes and meshes provide useful adjacent evidence but should not be conflated with building-envelope performance. TiO_2-WO_3@GO hollow-fiber membranes exhibit antifouling and catalytic memory in produced-water treatment [87], and TiO_2 grown in situ on titanium mesh provides underwater-superoleophobic oil–water separation [88]. These systems demonstrate the value of immobilization, hierarchical transport pathways, and in situ growth, but continuous immersion, forced flow, and contaminant transport differ fundamentally from intermittent sunlight, rain, abrasion, and dry deposition on facades. Their relevance here is therefore mechanistic rather than a direct demonstration of outdoor coating durability.

The Table 2 also illustrates why a single ranking of formulations is not meaningful. A four-year optical or power-retention record on glass, a salt-crystallization test on stone, and abrasion retention on concrete answer different service questions. The required performance envelope must be defined at the substrate–coating–exposure level.

Table 2. Substrate-specific design requirements and representative performance evidence for TiO_2-based building coatings.

Substrate/Service	Representative Coating Strategy	Reported Performance	Durability Evidence or Principal Constraint	Ref.
Concrete facade	TiO_2–SiO_2 hydrosol surface layer	72% MB degradation in 5 min and complete discoloration in 30 min under the reported UV test	Stable activity through 17 pull-off cycles and 6 h water impact; resistance to UV aging and acid exposure	[20]
Cementitious surface	TiO_2 coating applied before final setting	Retained photocatalytic performance with simultaneous matrix densification	Light-driven C-S-H/CH formation strengthened the interface and improved abrasion retention	[45]
Fly-ash/slag geopolymer	SiO_2-supported TiO_2 nano-architecture	74.98% NO_x removal in 60 min; 79.65% RhB degradation in 84 h before aging	79.35% RhB degradation after combined UV aging and rain scouring; compressive-strength gain	[68]
Friable carbonate stone	Pore-forming TiO_2–SiO_2 consolidating nanocomposite	Self-cleaning plus consolidation with limited visual change	Stable for >30 salt-crystallization cycles versus powdering after 3 cycles when untreated	[5]
Urban limestone	Water-dispersed nanosized TiO_2	Better early color preservation	Activity fell to negligible final rates after 8 months owing to TiO_2 loss and salt-associated deactivation	[2]

Table 2. *Cont.*

Substrate/Service	Representative Coating Strategy	Reported Performance	Durability Evidence or Principal Constraint	Ref.
Glass/PV cover	TiO_2–SiO_2-PAA superhydrophilic coating	Average relative self-cleaning efficacy ~4% on glass for 3 years; 2.8% PV power gain	Outdoor monitoring for 1–4 years; response depended on substrate and application route	[8]
Architectural latex paint	Clear TiO_2/hybrid-binder topcoat	Self-cleaning without visible-color change at 33%–45% TiO_2	Protected the underlying latex in outdoor and accelerated weathering without a separate interlayer	[82]

5. Performance Metrics and Evaluation Methods

5.1. Wettability Metrics

Water contact angle (WCA) and sliding angle (SA) are the primary descriptors of the physical self-cleaning regime. Superhydrophilic coatings are characterized by WCA $\leq 10^\circ$ or complete spreading (0°) [13,21,22,54], whereas superhydrophobic coatings target WCA > 150° and SA < 10° [23–26,47]. Photoinduced hydrophilicity is conventionally quantified by the decrease in WCA following UV exposure—for example, from ~84° to ~40° for Ca-TiO_2 [16], or to 9.8° for Cu-doped TiO_2 [14]. For self-healing or stimulus-responsive surfaces, the reversibility of the wetting state (e.g., recovery to superhydrophobicity after dark storage) is an additional figure of merit [46]. Contact-angle hysteresis is increasingly reported alongside static WCA, as it better reflects droplet mobility and the practical ease of self-cleaning [26,46].

Static WCA is nevertheless an incomplete descriptor. On rough or porous construction surfaces, absorption, pinning, evaporation, and droplet-size effects can make a single angle physically ambiguous. At minimum, advancing and receding angles or SA should accompany WCA for repellent coatings, while spreading time and illuminated-to-dark recovery should accompany WCA for superhydrophilic coatings. Measurements should be repeated at multiple locations and reported with dispersion because field-applied coatings are rarely uniform at the scale of a droplet. A photograph of a spherical droplet is not, by itself, evidence of low adhesion or self-cleaning.

5.2. Photocatalytic Dye Degradation

The discoloration of model organic dyes—methylene blue (MB), methyl orange (MO), and Rhodamine B (RhB)—is the most common laboratory proxy for photocatalytic self-cleaning. Reported efficiencies span a wide range depending on dye, catalyst loading, light source, and duration: 80% MB degradation by nanocrystalline anatase [34]; 96% MO decolorization by fluorocarbon/TiO_2-SiO_2 [78]; 97.08% MB by Ce-doped TiO_2 under visible light [17]; ~97% RhB by Ca-TiO_2 under simulated solar light [16]; and 88.81% MB by VO_2@Fe_2O_3–TiO_2 under visible light [18]. The choice of dye is itself consequential, since dyes differ in adsorption affinity, photostability, and susceptibility to sensitization, which can confound the attribution of discoloration to photocatalysis versus dye sensitization [10,29].

For a solution-phase test, removal is usually expressed as $\eta = (C_0 - C_t)/C_0 \times 100\%$, and an apparent pseudo-first-order constant is obtained from $\ln(C_0/C_t) = k_{app}t$ when the kinetic assumptions are supported. Neither quantity is intrinsic to a coating: k_{app} changes with illuminated area-to-volume ratio, photon flux, mass transfer, adsorption, and dye concentration. Dark adsorption and direct-photolysis controls are therefore mandatory.

For colored stains on a solid substrate, color difference (preferably CIE ΔE^*_{ab} or ΔE_{00}), residual stained area, and runoff-assisted removal are more service-relevant than solution concentration. Mineralization or byproduct analysis is needed before "degradation" is described as complete.

5.3. Air Depollution: NO_x, VOC, and Particulate Matter

Beyond aesthetic self-cleaning, TiO_2 coatings remove gaseous pollutants, extending their value to air purification. Nitrogen oxides (NO_x) are the most widely used inorganic probe: SiO_2-supported TiO_2 geopolymers achieved 74.98% NO_x removal [68]; Cu-TiO_2/SiO_2 and Au-TiO_2/SiO_2 coatings demonstrated enhanced NO removal [12,40]; and a sodium-laurate-modified coating degraded 99.1% NO [24]. Volatile organic compounds (VOCs) are degraded by coatings such as PMHS/TBT-DE-TiO_2, which removed over 99% of CH_2O and total VOC within 10,000 s and over 94% of PM2.5/PM10 within 600 s [89]. For indoor air, CuBTC/TiO_2/PS nanofibers electrospun onto HEPA filters achieved 98.6% toluene adsorption and 99.82% PM2.5 filtration with self-cleaning regeneration [90], and phenyl carbon nitride/TiO_2 coatings degraded wood- and cigarette-smoke residues (76.8% and 68.5%, respectively) under white LED light [91].

Gas-phase percentages require particular caution. Conversion depends on inlet concentration, relative humidity, flow rate, residence time, exposed area, and irradiance, and it can be inflated by adsorption if steady state is not reached. For NO_x, nitrate selectivity and the balance among NO, NO_2, and total NO_x should be reported because partial oxidation of NO to the more harmful NO_2 is not equivalent to purification. Area-normalized removal rate and photon-normalized efficiency are more transferable than conversion alone. Likewise, particle removal by a fibrous filter is governed primarily by filtration and pressure drop; it should not be presented as direct evidence that a passive wall coating will remove ambient particulate matter.

The evidence should be separated into three levels: (i) laboratory photocatalytic activity measured under a defined reactor condition; (ii) in situ activity of the deployed coating measured on the same surface after application; and (iii) a measurable change in ambient pollutant concentration or exposure. Evidence regarding immobilized TiO_2-containing HEPA filters under forced flow is retained strictly as adjacent context; its filtration and regeneration performance must not be extrapolated to suggest that passive building-envelope coatings can remove ambient particulate matter. This distinction is essential, as high laboratory conversion rates often fail to reflect field conditions where treated area-to-air volume ratios, pollutant transport dynamics, meteorology, and irradiance are fundamentally different.

For real-scale depollution, a pseudo-first-order constant normalized to radiant power can help parameterize surface kinetics, but it does not by itself establish improved urban air quality. The PhotoPAQ model-street-canyon campaign reported no statistically significant reductions in NO_x, O_3, VOCs, or particles and estimated an upper NO_x-remediation effect of about 2%. A later full-scale urban study likewise found no clear ambient NO_x improvement attributable to a TiO_2-treated road, whereas an earlier pilot-canyon experiment reported larger reductions under different transport and exposure conditions. These contrasting outcomes support cautious claims and require simultaneous measurement of pollutant concentrations, meteorology, traffic or emission conditions, treated area, and exposure duration.

5.4. Antimicrobial Activity

The ROS generated by illuminated TiO_2 also inactivate microorganisms, enabling simultaneous self-cleaning and antimicrobial surfaces. TiO_2-functionalized surfaces reduced

Staphylococcus aureus and Pseudomonas putida viability and biofilm formation [92]; Ag-TiO_2/PDMS coatings combined self-cleaning with photo-killing activity [76]; and Cu_2O/TiO_2 coatings achieved >99% sterilization of E. coli and S. aureus under visible light, retaining >90% bactericidal activity after 50 cycles [19]. Cu-doped TiO_2 showed superior E. coli inactivation compared with pure and Fe-doped TiO_2 [14], and Ag-doped TiO_2 wood coatings reduced E. coli colonization by 50% and eliminated S. aureus [84]. Cementitious composites incorporating nano-TiO_2 hydrogel exhibited light-dependent antibacterial activity, optimal at 2% loading [93]. Cu-doped TiO_2-SiO_2 nanocomposites prepared by a one-step sonochemical route likewise displayed composition-dependent antibacterial activity (inhibition zone) together with enhanced hydrophilicity [94].

Antimicrobial efficacy should preferably be reported as viable-count log reduction relative to both dark and illuminated uncoated controls. Percent reduction can obscure large differences in initial inoculum, and inhibition-zone tests confound contact killing with the leaching of Ag, Cu, or other soluble species. Organism, strain, inoculum, humidity, nutrient state, irradiance, exposure time, recovery method, and detection limit are required to distinguish photocatalysis from desiccation, heating, or metal-ion toxicity.

5.5. Standardized Tests and Their Limitations

A recurring conclusion of the recent literature is that standard laboratory tests imperfectly predict real-world performance. The accelerated degradation of a single dye under idealized illumination does not capture the multicomponent nature of environmental soiling, the role of rain and humidity, or the heterogeneity of real substrates [28–30]. Accordingly, several studies have introduced more realistic protocols: a customized artificial-soiling/rain-cycle procedure for heritage cement [29,30]; photodegradation of Rhodamine B as a surrogate for particulate matter [2,63]; soot degradation as a more realistic model of carbonaceous soiling [12,33,40]; and self-cleaning tests on glass [44]. Humidity is a particularly underappreciated variable: the stain-removal performance of porous and non-porous TiO_2 coatings is optimal at distinct relative humidities (35.1% and 53.4%, respectively), reflecting the interplay between surface hydration and photocatalytic activity [28]. The dependence of reported efficiencies on the model pollutant and protocol underscores the need for harmonized, substrate-specific, and weather-realistic test standards if self-cleaning coatings are to be benchmarked and commercialized on a reliable basis [1,28,30].

For coated glass, BS EN 1096-5:2016 [95] provides a dedicated test method and classification for self-cleaning properties. Its value is that the claim is tied to a defined coated-glass substrate, soiling procedure, illumination, rinsing step, and classification rather than to an isolated visual impression. For gaseous NO removal, ISO 22197-1:2016 [96] provides a standardized photocatalytic air-purification procedure, but its reactor result should be reported as surface activity and should not be presented as proof of an ambient air-quality benefit. Together with substrate-specific abrasion, weathering, and rain-scouring protocols, these standards can make the term self-cleaning more reproducible and prevent direct comparison of incompatible endpoints.

5.6. In Situ and Field Evaluation

Laboratory retesting after exposure is useful but does not fully represent the activity of a coating on the building surface. Portable continuous-flow photoreactors provide a practical bridge: Pellegrino et al. developed a portable device for rapid on-site measurement of photocatalytic surfaces using gaseous probes such as NO, including rough surfaces. Repeated measurements on the same exposed panel or facade area can track activity loss while preserving the local substrate, orientation, and weathering history. A field protocol should record irradiance, temperature, relative humidity, surface moisture, airflow, pollu-

tant concentration, exposed area, and any cleaning intervention, and should pair the activity result with adhesion, appearance, wettability, and nanoparticle-release measurements.

6. Outdoor Durability and Weathering

Long-term outdoor performance—rather than initial activity—is the decisive criterion for the adoption of self-cleaning coatings, yet it remains the least systematically characterized aspect of the field.

Outdoor durability is the retention of a defined function under a quantified exposure, not simply the absence of visible delamination. A coating can remain attached while losing accessible TiO_2 through fouling, salt coverage, surface reconstruction, or encapsulation by migrated polymer. Conversely, a modest decline in dye rate may accompany unacceptable haze, color change, water uptake, or nanoparticle release. Durability must therefore be assessed as coupled functional, mechanical, optical, chemical, and environmental retention.

6.1. Deactivation and Photocatalyst-Loss Mechanisms

Field studies consistently reveal a progressive decay of photocatalytic efficiency that is attributable to two coupled phenomena: the physical loss of the photocatalyst from the coating and its chemical deactivation. On limestone coated with a TiO_2/fluoropolymer nanocomposite exposed for one year in an urban environment, the photocatalytic efficiency of Rhodamine B degradation decreased progressively, an effect attributed to photocatalyst loss caused by polymer aging rather than to a reduction in intrinsic activity [4]. Similarly, water-dispersed TiO_2 coatings on limestone preserved surface color early in exposure but lost self-cleaning efficiency after eight months, a decline ascribed to both partial titania loss and deactivation by adsorbed soluble salts (either deposited from the atmosphere or produced by photocatalytic oxidation of pollutants) [2]. The accumulation of soluble ions is itself a concern because it may elevate the risk of salt-related stone damage [2,4].

Figure 5 presents an author-generated durability framework that separates environmental stressors, qualitative function-retention behavior, and field-monitoring outcomes. The curves in panel (b) are conceptual and do not reproduce experimental measurements; they illustrate how anchoring, porosity, and polymer shielding can produce different degradation trajectories. Panel (c) links repeated field inspection to the coupled loss mechanisms reported in Refs. [1,4].

The coating microstructure strongly modulates leaching and durability. Compact (dense) TiO_2 coatings with moderate activity exhibited minimal nanoparticle release and were deemed suitable for domestic applications, whereas initially highly active mesoporous coatings suffered a dramatic drop in self-cleaning performance and a significant release of nanoparticles upon exposure to common household chemicals [1]. This finding has direct implications for human health and environmental safety, since weathering-induced nanoparticle release is an emerging regulatory concern [1,60].

Five recurring failure modes can be distinguished. First, cohesive loss removes active material through rain impact, abrasion, or dissolution of the surrounding binder. Second, adhesive failure cracks or delaminates the film at the substrate interface. Third, chemical poisoning or masking covers active sites with salts, dust, reaction products, or organic residues. Fourth, photo-oxidation embrittles an organic binder or destroys a low-surface-energy modifier. Fifth, roughness collapse, pore flooding, or surface reconstruction changes the wetting state even when composition appears unchanged. These modes can interact: ROS-mediated binder oxidation exposes particles, which are subsequently released by rain, while the resulting roughness and chemistry shift the WCA. Post-aging microscopy, surface chemistry, mass balance, leachate analysis, and functional testing are therefore complementary rather than interchangeable.

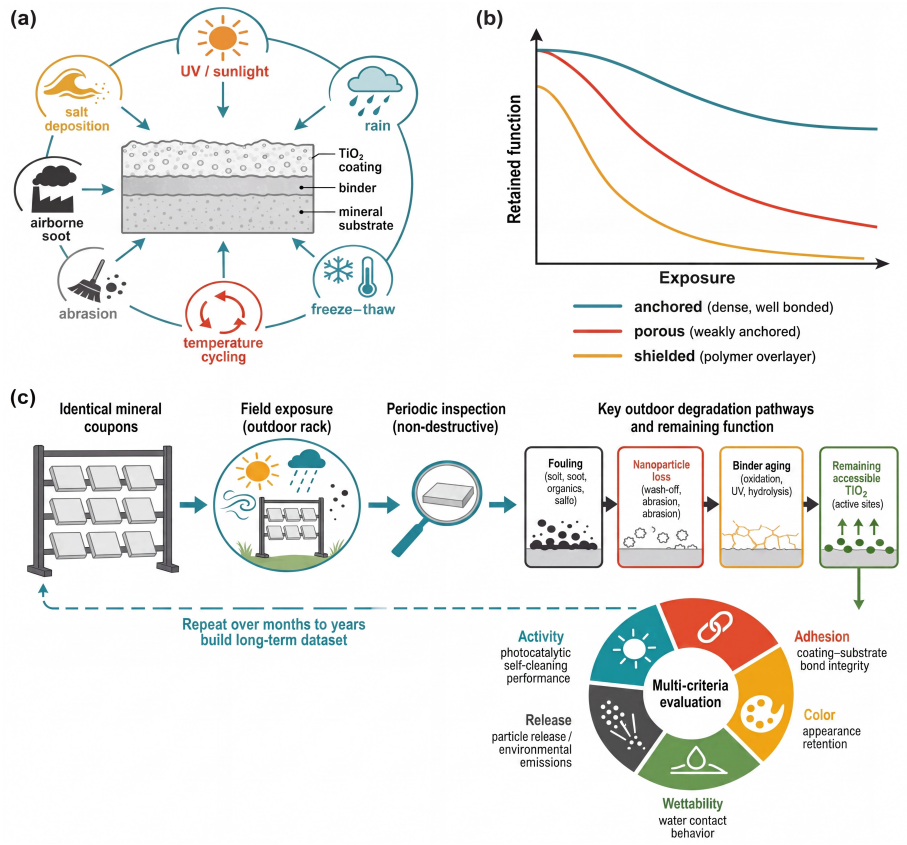


Figure 5. Original framework for evaluating outdoor durability rather than a reproduction of measured data: (**a**) principal environmental stressors acting on a coated mineral substrate; (**b**) qualitative performance-retention trajectories for different coating architectures (schematic only); and (**c**) a field-exposure workflow linking repeated inspection to fouling, nanoparticle loss, binder aging, residual TiO_2 accessibility, and multi-criteria performance. Drawn by the authors based on durability findings discussed in Refs. [1,4].

6.2. Substrate-Dependent Aging and UV Resistance

Durability cannot be extrapolated across substrates, since photocatalytic stability depends on substrate morphology and nature [31]. TiO_2 coatings on fired clay brick facades retained stable photocatalytic efficiency after UV exposure and wet–dry cycling, remaining seven-fold more effective than untreated bricks in the long term [31]. On limestone, the preservation of nanostructured coatings depends on both film characteristics (crack-free versus fissured) and substrate roughness and cohesion; crack-free, conformable films anchored well to both compact and soft limestones, whereas fissured films on compact limestone underwent adhesion failure and activity loss [32]. Organic binder matrices are a common weak point: fluorocarbon/TiO_2-SiO_2 coatings were markedly more UV-stable than TiO_2-filled fluorocarbon coatings, indicating that the silica component mitigates binder photodegradation [78], and inorganic or sericite-based UV-shielding carriers protect hydrophobic modifiers from photo-oxidation [47]. Fluorine-free superhydrophobic coatings maintained superhydrophobicity for 6 months outdoors [25], while a PVDF-TiO_2-HAP coating performed satisfactorily after 8000 h of outdoor service [9].

6.3. Long-Term and Field Studies

Quantitative long-term data are scarce but essential. A TiO_2–SiO_2-PAA coating was monitored outdoors for up to four years on glass and PET, revealing substrate-dependent relative self-cleaning efficacy (stabilizing at ~15% on PET after 150 days; ~4% on glass for three years before declining to ~2% in year four) and a 2.8% gain in PV power generation [8].

TiO_2/SiO_2-coated concrete retained essentially unchanged structure and photocatalytic efficacy after four months of real exposure and repeated degradation cycles [33]. In contrast, a one-year urban-exposure study of TiO_2/fluoropolymer-coated limestone documented the progressive loss described above [4], and a parallel study recorded negligible final self-cleaning rates after eight months [2]. These results collectively indicate that durability is governed by the substrate–binder–photocatalyst triad and that inorganic or silica-rich matrices generally outperform organic ones under prolonged weathering [8,20,33,68].

Durability qualification should therefore include periodic in situ photocatalytic measurements on the same exposed surface, rather than relying only on dye discoloration or laboratory coupons prepared after weathering. The activity record should be synchronized with cumulative UV dose, rainfall, temperature and humidity cycles, salt deposition, particulate loading, and cleaning events. This approach would reveal whether an apparent decline reflects loss of accessible TiO_2, temporary fouling, changes in surface wetting, or irreversible chemical deactivation.

Table 3 summarizes representative outdoor-exposure and weathering results for TiO_2-based coatings applied to different building substrates. The reported results indicate that functional retention is strongly dependent on the substrate–binder–photocatalyst combination and the exposure environment. Silica-rich and inorganic coating architectures generally exhibit improved resistance to UV irradiation, rain scouring, and photocatalyst loss, whereas coatings applied to limestone with water-dispersed TiO_2 or fluoropolymer binders may experience progressive deactivation associated with salt deposition, binder aging, and catalyst loss.

Table 3. Representative outdoor and weathering evidence, arranged by exposure duration and endpoint.

Coating/Substrate	Exposure	Endpoint and Outcome	Interpretive Limitation	Ref.
Water-dispersed TiO_2 on limestone	8 months, urban outdoor exposure	Early color preservation was lost; self-cleaning reached negligible final rates; partial Ti loss and soluble salts implicated	One stone/coating/environment; RhB-based endpoint	[2]
TiO_2/fluoropolymer on limestone	1 year, urban outdoor exposure	Progressive reduction in hydrophobic and photocatalytic performance, with composition-dependent residual activity	Polymer aging, deposition, and Ti loading changed concurrently	[4]
TiO_2/SiO_2 on concrete	4 months outdoors plus repeated MB cycles	Structure and photocatalytic efficacy were reported as essentially retained	Shorter field duration than facade service life	[33]
A-SiO_2/N-TiO_2@HDTMS on rigid substrates	3 months outdoors	Self-cleaning and recoverable superhydrophobicity retained	Short exposure and no direct facade load history	[46]
Fluorine-free PDMS/EP/STA/TiO_2	6 months outdoors plus laboratory abrasion	Superhydrophobic state retained after reported tape/sandpaper tests	Polymer-rich coating; site climate and cumulative UV/rain dose govern transferability	[25]

Table 3. *Cont.*

Coating/Substrate	Exposure	Endpoint and Outcome	Interpretive Limitation	Ref.
PVDF-TiO_2-HAP on an architectural louver	8000 h/ approximately 1 year outdoors	Satisfactory hydrophilicity and self-cleaning reported under natural exposure	Performance assessed on a specific geometry and climate	[9]
TiO_2–SiO_2-PAA on glass, PET, and PV modules	1–4 years outdoors	Substrate-dependent relative self-cleaning efficacy (RSCE); ~4% average on glass for 3 years, ~2% in year 4; 2.8% PV power gain	RSCE is an optical/service metric, not a photocatalytic rate	[8]

6.4. Strategies to Enhance Outdoor Durability

Several design principles have emerged for durable coatings. First, inorganic binders and cohesive silica networks improve adhesion and resist photodegradation: SiO_2-supported TiO_2 on geopolymer retained 79.35% RhB degradation after UV aging and rain scouring (2.8-fold better than pure nano-TiO_2) [68], and TiO_2–SiO_2 hydrosol coatings endured 17 pull-off cycles, 6 h of water impact, UV aging, and acid exposure [20]. Second, light-driven hydration can strengthen the coating–cement interface: a TiO_2 coating applied before cement setting promoted the nucleation of hydration products (C-S-H and CH) at the interface through photoinduced hydroxylation, yielding coatings that retained photocatalytic performance after mechanical abrasion while simultaneously densifying and strengthening the matrix [45]. Third, the co-optimization of TiO_2 loading and binder chemistry avoids both photocatalytic attack on the binder and excessive photocatalyst content—clear TiO_2/silane topcoats (33%–45% TiO_2) protected the underlying latex from UV damage while remaining self-cleaning [82]. Fourth, defect and heterojunction engineering simultaneously improves visible-light activity and, by reducing reliance on organic sensitizers, potentially improves long-term stability [16,43,44]. Finally, the adoption of weathering-realistic and nanoparticle-release-aware testing protocols is itself a prerequisite for developing coatings that are both durable and environmentally benign [1,29,30].

The examples also qualify the common assumption that inorganic content automatically ensures durability. Silica can improve cohesion and shield a polymer, but a brittle silica-rich film may crack on a dimensionally active substrate; defect engineering can increase activity while also increasing adsorption or chemical reactivity; and a highly porous architecture can maximize initial rate while accelerating contaminant ingress and particle release. Durable design is consequently an optimization of controlled accessibility, not maximum exposed surface area.

6.5. From Accelerated Aging to Service-Life Qualification

A useful qualification sequence should proceed from isolated stressors to coupled exposures. Initial screening can measure adhesion, abrasion, water impact, UV stability, acid/alkali resistance, and freeze–thaw or salt crystallization separately. A second tier should combine UV, humidity, temperature cycling, deposited model soil, and simulated rain because the order of stresses matters: UV may embrittle a binder before rain removes particles, while salts may crystallize during drying after a wet period. The final tier should use replicated outdoor panels at relevant orientations, with uncoated and commercial controls, periodic cleaning events, and climate-dose records. Accelerated tests should be calibrated against the same failure mode observed outdoors rather than justified only by a high lamp intensity.

At each tier, both absolute performance and retention should be reported. For a beneficial quantity such as rate or transmittance gain, $R_f = P_{aged}/P_{initial}$ is intuitive; for

quantities where lower is better, such as sliding angle or color change, the raw before/after values are clearer. Failure criteria should be declared before testing and should include adhesion, visual compatibility, water transport, functional retention, and Ti release. This framework would permit claims such as "retained 80% of initial area-normalized NO_x removal after a defined UV–rain cycle with Ti release below a stated mass per area," which is substantially more informative than "excellent weather resistance."

7. Conclusions and Outlook

TiO_2-based coatings have reached a high degree of maturity as self-cleaning, depolluting, and antimicrobial treatments for building materials. The mechanistic basis is now well established: photocatalytic mineralization by photogenerated reactive oxygen species is complemented by photoinduced superhydrophilicity, and, in increasingly prevalent dual-functional systems, by engineered superhydrophobic or superamphiphobic wetting states that physically shed contaminants. Material design has progressed from pristine anatase through morphology and facet engineering, SiO_2–TiO_2 composites, and metal/non-metal doping and heterojunctions for visible-light activation, to carbon-based and microencapsulated hybrids, with demonstrated compatibility across cementitious substrates, natural stone and heritage materials, and transparent glass and photovoltaic surfaces.

Nevertheless, several open challenges must be resolved before these coatings can be deployed at scale with confidence. First, the field lacks harmonized, substrate-specific, and weather-realistic evaluation protocols; the prevailing reliance on idealized single-dye discoloration understates the complexity of real soiling and hinders comparison across studies. Second, outdoor durability remains under-demonstrated: field and accelerated-weathering studies repeatedly show that photocatalytic efficiency decays through photocatalyst loss, deactivation by soluble salts, and UV degradation of organic matrices, and that performance cannot be extrapolated across substrates. Third, the environmental dimension—particularly the weathering-induced release of photocatalytic nanoparticles—deserves systematic investigation alongside regulatory frameworks. Fourth, the tension between visible-light activity and long-term stability, and between superhydrophobicity and photodegradation of the (often organic) low-surface-energy modifiers, calls for inorganic, defect-engineered, and heterojunction-based solutions that do not trade durability for initial performance.

Looking forward, the most promising directions include (i) defect- and heterojunction-engineered photocatalysts that deliver visible-light activity from earth-abundant elements; (ii) inorganic and silica-rich binder chemistries, including light-driven hydration strategies, that strengthen coating–substrate interfaces; (iii) fluorine-free, self-healing repellent systems; (iv) the integration of self-cleaning with complementary functionalities such as radiative-cooling, thermal comfort, and energy generation; and (v) the establishment of standardized outdoor-aging and nanoparticle-release test methods. Addressing these challenges will determine whether TiO_2-based self-cleaning coatings fulfill their considerable promise as durable, low-maintenance, and environmentally beneficial components of the built environment.

Author Contributions: Y.L.: Conceptualization, Supervision, Investigation, Writing—Draft, Writing—Reviewing and Editing, S.L.: Investigation, Writing—Reviewing and Editing, Z.H.: Investigation, Writing—Reviewing and Editing, T.D.: Investigation, Writing—Reviewing and Editing. All authors have read and agreed to the published version of the manuscript.

Funding: This research was funded by the Taizhou Science and Technology Plan Project (Project No.: 25gb31); General Projects of the Department of Education of Zhejiang Province (Project No.: Y202558551); The Research Start-up Fund for High-level Talents of Taizhou Vocational & Technical College (Project No.: 2025GCC06).

Institutional Review Board Statement: Not applicable.

Informed Consent Statement: Not applicable.

Data Availability Statement: No new data were created or analyzed in this study. Data sharing is not applicable to this article.

Acknowledgments: During the preparation of this manuscript, the authors used ChatGPT (GPT-5.5, OpenAI) for the purposes of language polishing and improving the grammar, clarity, and readability of the text.

Conflicts of Interest: The authors declare no conflicts of interest.

References

1. Cedillo-González, E.I.; Barbieri, V.; Falcaro, P.; Torres-Martínez, L.M.; Juárez-Ramírez, I.; Villanova, L.; Montecchi, M.; Pasquali, L.; Siligardi, C. Influence of domestic and environmental weathering in the self-cleaning performance and durability of TiO_2 photocatalytic coatings. *Build. Environ.* **2018**, *132*, 96–103. [CrossRef]
2. Lettieri, M.; Colangiuli, D.; Masieri, M.; Calia, A. Field performances of nanosized TiO_2 coated limestone for a self-cleaning building surface in an urban environment. *Build. Environ.* **2019**, *147*, 506–516. [CrossRef]
3. Gholami, Z.; Jalilisadrabad, S.; Amrollahi, R. Investigating the impact of using modified cool materials by titanium dioxide (TiO_2)-based photocatalytic self-cleaning nanoparticles in urban facades on urban microclimate parameters. *Case Stud. Constr. Mater.* **2023**, *19*, e02268. [CrossRef]
4. Colangiuli, D.; Lettieri, M.; Masieri, M.; Calia, A. Field study in an urban environment of simultaneous self-cleaning and hydrophobic nanosized TiO_2-based coatings on stone for the protection of building surface. *Sci. Total Environ.* **2019**, *650*, 2919–2930. [CrossRef]
5. Pinho, L.; Elhaddad, F.; Facio, D.S.; Mosquera, M.J. A novel TiO_2–SiO_2 nanocomposite converts a very friable stone into a self-cleaning building material. *Appl. Surf. Sci.* **2013**, *275*, 389–396. [CrossRef]
6. Calia, A.; Lettieri, M.; Masieri, M.; Pal, S.; Licciulli, A.; Arima, V. Limestones coated with photocatalytic TiO_2 to enhance building surface with self-cleaning and depolluting abilities. *J. Clean. Prod.* **2017**, *165*, 1036–1047. [CrossRef]
7. Huang, R.; Zhou, T.; Lu, Q.; Hu, L.; Liu, P.; Hu, B.; Wang, L.; Wang, X. Research on the application of anti-reflective self-cleaning technology in photovoltaic panels. *Sol. Energy Mater. Sol. Cells* **2026**, *294*, 113920. [CrossRef]
8. Yang, L.; Yang, J.; Yang, D.-Q. A durable superhydrophilic self-cleaning coating based on TiO_2–SiO_2-PAA nanocomposite for photovoltaic applications: Long-term outdoor study. *Sol. Energy Mater. Sol. Cells* **2024**, *268*, 112731. [CrossRef]
9. Wu, S.; Li, L.; Jiang, T.; Gui, Y.; Song, K.; Li, J.; Ma, D.; Zhang, Y.; Liang, L.; Zhang, Z.; et al. Excellent self-cleaning surface achieved through the synergistic effect of superhydrophilicity and photocatalysis of PVDF-TiO_2-HAP coating. *Surf. Interfaces* **2024**, *51*, 104676. [CrossRef]
10. Bergamonti, L.; Predieri, G.; Paz, Y.; Fornasini, L.; Lottici, P.P.; Bondioli, F. Enhanced self-cleaning properties of N-doped TiO_2 coating for Cultural Heritage. *Microchem. J.* **2017**, *133*, 1–12. [CrossRef]
11. Kaveh, R.; Alijani, H.; Falletta, E.; Bianchi, C.L.; Mokhtarifar, M.; Boffito, D.C. Advancements in superhydrophilic titanium dioxide/graphene oxide composites coatings for self-cleaning applications on glass substrates: A comprehensive review. *Prog. Org. Coat.* **2024**, *190*, 108347. [CrossRef]
12. Luna, M.; Mosquera, M.J.; Vidal, H.; Gatica, J.M. Au-TiO_2/SiO_2 photocatalysts for building materials: Self-cleaning and de-polluting performance. *Build. Environ.* **2019**, *164*, 106347. [CrossRef]
13. Bento, D.H.; Matias, M.L.; Magalhães, M.; Quitério, C.; Pimentel, A.; Sousa, D.; Amaral, P.; Galhano, C.; Fortunato, E.; Martins, R.; et al. Self-cleaning stone Façades using TiO_2 Microwave-Synthesised Coatings. *Clean. Mater.* **2025**, *15*, 100294. [CrossRef]
14. Mehmandoustesfahani, E.; Hakimi, F.; Rodríguez-Chueca, J.; Díaz–López, J.A.; Nieto–Márquez, A. Visible-light-activated Cu and Fe-doped TiO_2 thin films on glass: Photocatalytic, antibacterial and self-cleaning performance. *Open Ceram.* **2026**, *25*, 100916. [CrossRef]
15. Miljević, B.; van der Bergh, J.M.; Vučetić, S.; Lazar, D.; Ranogajec, J. Molybdenum doped TiO_2 nanocomposite coatings: Visible light driven photocatalytic self-cleaning of mineral substrates. *Ceram. Int.* **2017**, *43*, 8214–8221. [CrossRef]
16. Li, X.; Huang, Q.; Liu, L.; Zhu, W.; Elkhooly, T.A. Reduced inflammatory response by incorporating magnesium into porous TiO_2 coating on titanium substrate. *Colloids Surf. B Biointerfaces* **2018**, *171*, 276–284. [CrossRef]
17. Gadge, A.S.; Janbandhu, S.Y.; Gedam, R.S. Exploring the photocatalytic and antibacterial activity of Ce-doped TiO_2 nanoparticles with remarkable self-cleaning superhydrophilic surface for outdoor application. *Ceram. Int.* **2025**, *51*, 602–611. [CrossRef]
18. Nzangue Fobasso, L.A.; Lukong, V.T.; Nkwachukwu, O.V.; Jen, T.-C. Sol-gel synthesized VO_2@Fe_2O_3–TiO_2 nanocomposite for improved photocatalytic and self-cleaning performance. *J. Sci. Adv. Mater. Devices* **2025**, *10*, 101017. [CrossRef]

19. Matías, E.; Aguirre, Z.R.; Eugene, A.J.; Guzman, M.I.; María, A.G. Cu_2O/TiO_2 heterostructures for CO_2 reduction through a direct Z-scheme: Protecting Cu_2O from photocorrosion. *Appl. Catal. B Environ.* **2017**, *217*, 485. [CrossRef]
20. Cetinkaya, T.; Neuwirthova, L.; Kutlakova, K.M.; Tomasek, V.; Akbulut, H. Synthesis of nanostructured TiO_2/SiO_2 as an effective photocatalyst for degradation of acid orange. *Appl. Surf. Sci.* **2013**, *279*, 384–390. [CrossRef]
21. Jundle, A.R.; Ekunde, R.A.; Khutale, S.N.; Rashivade, S.R.; Bansode, T.S.; Sidharaddi, R.S.; Sutar, R.S.; Liu, S.; Latthe, S.S. Sol-gel processed superhydrophilic TiO_2–SiO_2 coatings on marble for outdoor photocatalytic self-cleaning application. *Ceram. Int.* **2026**, *52*, 40264–40278. [CrossRef]
22. Wang, X.; Ding, H.; Lv, G.; Zhou, R.; Ma, R.; Hou, X.; Zhang, J.; Li, W. Fabrication of superhydrophilic self-cleaning SiO_2–TiO_2 coating and its photocatalytic performance. *Ceram. Int.* **2022**, *48*, 20033–20040. [CrossRef]
23. Liao, G.; Yao, W.; She, A.; Bian, X. An eco-friendly building coating with high self-cleaning capacity: Synergetic effect of super-hydrophobicity and photocatalytic degradation. *Constr. Build. Mater.* **2023**, *406*, 133406. [CrossRef]
24. Zhan, L.; Wang, G.; Huang, B.; Liu, F.; Qu, F.; Zhu, M. Dual-functional coating: Synergistic photocatalysis and superhydrophobicity with persistent weathering resistance for self-cleaning concrete. *Surf. Interfaces* **2026**, *80*, 108290. [CrossRef]
25. Zhao, Y.; Liu, M.; Zhao, M.; Liu, J.; Zhang, X. Fabricating a fluorinated-free superhydrophobic PDMS/EP/STA/TiO_2 coating with photocatalytic and durable properties via a one-step spraying method. *Vacuum* **2025**, *242*, 114757. [CrossRef]
26. Zhang, L.; Li, R.; Ding, H.; Chen, D.; Wang, X. Preparation of a self-cleaning TiO_2-SiO_2/PFDTS coating with superamphiphobicity and photocatalytic performance. *Prog. Org. Coat.* **2024**, *197*, 108767. [CrossRef]
27. Manoudis, P.N.; Zuburtikudis, I.; Khalifeh, H.A.; Karapanagiotis, I. Robust and transparent smooth amphi-repellent coating with physical self-cleaning and photocatalytic activities. *Surf. Interfaces* **2024**, *52*, 104928. [CrossRef]
28. Cedillo-González, E.I.; Hernández-López, J.M.; Ruiz-Valdés, J.J.; Barbieri, V.; Siligardi, C. Self-cleaning TiO_2 coatings for building materials: The influence of morphology and humidity in the stain removal performance. *Constr. Build. Mater.* **2020**, *237*, 117692. [CrossRef]
29. Artale, A.; Fregni, A.; Franzoni, E. About the self-cleaning potential of TiO_2-TEOS treatments for heritage cementitious materials. *Constr. Build. Mater.* **2025**, *496*, 143735. [CrossRef]
30. Franzoni, E.; Pizzigatti, C.; Fabris, R. Developing inorganic coatings with nano-TiO_2 for heritage concrete and assessing their self-cleaning performance by a new laboratory test. *Constr. Build. Mater.* **2024**, *449*, 138282. [CrossRef]
31. Graziani, L.; Quagliarini, E.; Bondioli, F.; D'Orazio, M. Durability of self-cleaning TiO_2 coatings on fired clay brick façades: Effects of UV exposure and wet & dry cycles. *Build. Environ.* **2014**, *71*, 193–203. [CrossRef]
32. Calia, A.; Lettieri, M.; Masieri, M. Durability assessment of nanostructured TiO_2 coatings applied on limestones to enhance building surface with self-cleaning ability. *Build. Environ.* **2016**, *110*, 1–10. [CrossRef]
33. Khannyra, S.; Luna, M.; Gil, M.L.A.; Addou, M.; Mosquera, M.J. Self-cleaning durability assessment of TiO_2/SiO_2 photocatalysts coated concrete: Effect of indoor and outdoor conditions on the photocatalytic activity. *Build. Environ.* **2022**, *211*, 108743. [CrossRef]
34. Yun, H.; Nguyen-Phan, T.-D.; Pham, V.H.; Kweon, H.; Chung, J.S.; Lee, B.; Shin, E.W. Influence of TiO_2 dimension and graphene oxide content on the self-cleaning activity of methylene blue-stained photocatalytic films. *Mater. Res. Bull.* **2012**, *47*, 2988–2993. [CrossRef]
35. Luna, M.; Delgado, J.J.; Romero, I.; Montini, T.; Almoraima Gil, M.L.; Martínez-López, J.; Fornasiero, P.; Mosquera, M.J. Photocatalytic TiO_2 nanosheets-SiO_2 coatings on concrete and limestone: An enhancement of de-polluting and self-cleaning properties by nanoparticle design. *Constr. Build. Mater.* **2022**, *338*, 127349. [CrossRef]
36. Yang, J.; Wang, G.; Wang, D.; Liu, C.; Zhang, Z. A self-cleaning coating material of TiO_2 porous microspheres/cement composite with high-efficient photocatalytic depollution performance. *Mater. Lett.* **2017**, *200*, 1–5. [CrossRef]
37. Besleaga, C.; Tomulescu, A.G.; Zgura, I.; Stepanova, A.; Galca, A.C.; Laafar, S.; Zorila, F.L.; Alexandru, M.; Pintilie, I.; Iliescu, M. Reticulated mesoporous TiO_2 scaffold for self-cleaning surfaces. *Ceram. Int.* **2024**, *50*, 42264–42275. [CrossRef]
38. Kumar, A.; Nayak, D.; Nandi, B.K.; Saxena, V.K.; Thangavel, R. Visible light active and self-cleaning SiO_2/N-TiO_2 heterostructure surface with high transmittance for solar module glass cover: Experimental and DFT insights. *J. Environ. Chem. Eng.* **2023**, *11*, 111117. [CrossRef]
39. Pinho, L.; Rojas, M.; Mosquera, M.J. Ag–SiO_2–TiO_2 nanocomposite coatings with enhanced photoactivity for self-cleaning application on building materials. *Appl. Catal. B Environ.* **2015**, *178*, 144–154. [CrossRef]
40. Khannyra, S.; Mosquera, M.J.; Addou, M.; Gil, M.L.A. Cu-TiO_2/SiO_2 photocatalysts for concrete-based building materials: Self-cleaning and air de-pollution performance. *Constr. Build. Mater.* **2021**, *313*, 125419. [CrossRef]
41. Wu, D.; Wang, H.; Li, C.; Xia, J.; Song, X.; Huang, W. Photocatalytic self-cleaning properties of cotton fabrics functionalized with p-BiOI/n-TiO_2 heterojunction. *Surf. Coat. Technol.* **2014**, *258*, 672–676. [CrossRef]
42. Xu, L.; Meng, Y.; Zhao, Y.; Su, J.; Han, J. Durable self-cleaning PVDF coating with photocatalysis and superhydrophobic property based on hierarchical coral-like 2D g-C_3N_4/1D TiO_2 hybrid. *J. Environ. Chem. Eng.* **2023**, *11*, 109541. [CrossRef]

43. Cui, S.; Duan, Z.; Deng, H.; Luo, X.; Jia, Z.; Quan, W.; Wang, R.; Liu, Y.; Liu, D. Fabrication of micro-patterned Co^{2+}-TiO_2/$LaNiO_3$ direct Z-scheme heterojunction films via photosensitive sol-gel rinsing for self-cleaning applications. *Mater. Chem. Phys.* **2026**, *356*, 132341. [CrossRef]
44. Henríquez, A.; Melin, V.; Romero, R.; Murillo-Sierra, J.C.; Cerna, M.; Yáñez, V.; Salas, B.; Cornejo-Ponce, L.; Pecchi, G.; Contreras, D. Visible-Light activated self-cleaning glass using BiOI/TiO_2 nanocomposites. *Surf. Interfaces* **2025**, *65*, 106481. [CrossRef]
45. Liu, G.; Zhang, J.; Wu, J.; Zhan, Y.; Zhao, T.; Ma, Y.; Run, M.; Li, F.; Niu, X. Enhancement for photocatalytic durability and mechanical properties of TiO_2 coating on cement based-materials by light-driven hydration. *Constr. Build. Mater.* **2025**, *497*, 143885. [CrossRef]
46. Wang, X.; Ding, H.; Wang, C.; Zhou, R.; Li, Y.; Li, W.; Ao, W. Self-healing superhydrophobic A-SiO_2/N-TiO_2@HDTMS coating with self-cleaning property. *Appl. Surf. Sci.* **2021**, *567*, 150808. [CrossRef]
47. Zhang, L.; Liu, Y.; Wang, X.; Chen, D.; Ding, H. Fabrication of sericite-TiO_2/HDTMS superhydrophobic self-cleaning coatings by hydrothermal method. *J. Alloys Compd.* **2025**, *1014*, 178677. [CrossRef]
48. Batool, I.; Shahzad, N.; Shahzad, R.; Naseem Satti, A.; Liaquat, R.; Waqas, A.; Imran Shahzad, M. Self-cleaning study of SiO_2 modified TiO_2 nanofibrous thin films prepared via electrospinning for application in solar cells. *Sol. Energy* **2024**, *268*, 112271. [CrossRef]
49. Ismail, A.A.; Alzubi, F.; Al-Hajji, L.A.; Alseidi, M.; Ahmad, S.; Alduweesh, A. Self-cleaning coatings for minimizing the impact of dust precipitation on the power production of solar cells utilizing mesoporous TiO_2/SiO_2 and ZnO/SiO_2 films. *Ceram. Int.* **2023**, *49*, 22788–22796. [CrossRef]
50. Bai, X.; Yang, S.; Tan, C.; Jia, T.; Guo, L.; Song, W.; Jian, M.; Zhang, X.; Zhang, Z.; Wu, L.; et al. Synthesis of TiO_2 based superhydrophobic coatings for efficient anti-corrosion and self-cleaning on stone building surface. *J. Clean. Prod.* **2022**, *380*, 134975. [CrossRef]
51. Wu, J.; Wang, H.; Bao, L.; Zhong, J.; Chen, R.; Sun, L. Novel raspberry-like hollow SiO_2@TiO_2 nanocomposites with improved photocatalytic self-cleaning properties: Towards antireflective coatings. *Thin Solid Films* **2018**, *651*, 48–55. [CrossRef]
52. Li, Z.; He, H.; Wang, X.; Shou, C.; Huang, M.; Jin, S.; Du, X. Robust SiO_2@TiO_2 nanocoatings with antireflection and photocatalytic self-cleaning properties by introducing commercial P25 TiO_2. *Colloids Surf. A Physicochem. Eng. Asp.* **2023**, *664*, 131176. [CrossRef]
53. Azhari, N.; Chatchiangkan, C.; Barnthip, N.; Pavasupree, S. Enhancing the self-cleaning properties of ball-milled TiO_2 nanoparticles: Sustainable utilization of natural rutile and leucoxene from Thailand. *Case Stud. Constr. Mater.* **2025**, *23*, e05247. [CrossRef]
54. Adachi, T.; Latthe, S.S.; Gosavi, S.W.; Roy, N.; Suzuki, N.; Ikari, H.; Kato, K.; Katsumata, K.-i.; Nakata, K.; Furudate, M.; et al. Photocatalytic, superhydrophilic, self-cleaning TiO_2 coating on cheap, light-weight, flexible polycarbonate substrates. *Appl. Surf. Sci.* **2018**, *458*, 917–923. [CrossRef]
55. Ren, Y.; Li, W.; Cao, Z.; Jiao, Y.; Xu, J.; Liu, P.; Li, S.; Li, X. Robust TiO_2 nanorods-SiO_2 core-shell coating with high-performance self-cleaning properties under visible light. *Appl. Surf. Sci.* **2020**, *509*, 145377. [CrossRef]
56. Ansari, A.; Nouri, N.M. A one step self-cleaning surface with robust superhydrophobic and photocatalytic properties: Electrostatic sprayed fluorinated ethylene propylene mixed with nano TiO_2–SiO_2 particles. *Ceram. Int.* **2023**, *49*, 57–66. [CrossRef]
57. Srivastava, A.A.; Bondarev, V.P.; Kostyleva, E.I.; Novikov, A.N.; Fukina, D.G.; Markov, A.N.; Markin, Z.A.; Kazarina, O.V. Doped TiO_2 and oligoalkylhydrosiloxane-based surface modifiers with self-cleaning and hydrophobic properties. *Next Mater.* **2026**, *10*, 101414. [CrossRef]
58. Li, Z.; Zhao, X.; Zhang, H. Synergistic construction of h-BN/TiO_2-WO_3 ceramic coating and coral-like superamphiphobic surface for enhanced corrosion resistance and self-cleaning. *Surf. Interfaces* **2026**, *93*, 109496. [CrossRef]
59. Deepa, M.J.; Arunima, S.R.; Shibli, S.M.A. Hydrophobic and corrosion-resistant composite ($BiVO_4$/TiO_2) hot-dip zinc coating with enhanced self-cleaning ability. *J. Alloys Compd.* **2022**, *924*, 166522. [CrossRef]
60. Prudente, I.N.R.; Santos, H.C.d.; Fonseca, J.L.; de Almeida, Y.A.; Gimenez, I.d.F.; Barreto, L.S. Graphene family (GFMs), carbon nanotubes (CNTs) and carbon black (CB) on smart materials for civil construction: Self-cleaning, self-sensing and self-heating. *J. Build. Eng.* **2024**, *95*, 110175. [CrossRef]
61. Wang, X.; Ma, C.; Zou, F.; Hu, H.; Li, J.; Luo, H. $CaCO_3$/TiO_2 hybrid microcapsules with self-cleaning and self-repairing functions for decorative coatings. *Inorg. Chem. Commun.* **2024**, *159*, 111665. [CrossRef]
62. Ma, C.; Wang, X.; Zou, F.; Zhong, Y.; Guo, G. Preparation of TiO_2 hybrid SiO_2 wall environment-friendly microcapsules based on interfacial polycondensation: Realize the integration of self-cleaning and self-healing functions. *Mater. Today Commun.* **2024**, *41*, 111034. [CrossRef]
63. Krishnan, P.; Zhang, M.-H.; Yu, L.; Feng, H. Photocatalytic degradation of particulate pollutants and self-cleaning performance of TiO_2-containing silicate coating and mortar. *Constr. Build. Mater.* **2013**, *44*, 309–316. [CrossRef]
64. Wang, Z.; Gauvin, F.; Feng, P.; Brouwers, H.J.H.; Yu, Q. Self-cleaning and air purification performance of Portland cement paste with low dosages of nanodispersed TiO_2 coatings. *Constr. Build. Mater.* **2020**, *263*, 120558. [CrossRef]
65. Zhang, D.; Zhu, H.; Yang, Q.; Mao, M.; Li, J. Hydration kinetics, mechanical, and photocatalytic self-cleaning performance of permeable concrete reinforced with nano-TiO_2 hydrosol. *Constr. Build. Mater.* **2025**, *472*, 140830. [CrossRef]

66. Diamanti, M.V.; Del Curto, B.; Ormellese, M.; Pedeferri, M.P. Photocatalytic and self-cleaning activity of colored mortars containing TiO_2. *Constr. Build. Mater.* **2013**, *46*, 167–174. [CrossRef]
67. Li, Q.; Liu, Q.; Peng, B.; Chai, L.; Liu, H. Self-cleaning performance of TiO_2-coating cement materials prepared based on solidification/stabilization of electrolytic manganese residue. *Constr. Build. Mater.* **2016**, *106*, 236–242. [CrossRef]
68. Su, P.-C.; Sui, C.-E.; Yang, W.-J. Simultaneous enhancement of mechanical strength and photocatalytic durability in geopolymers via SiO_2-supported TiO_2 nano-architecture. *Case Stud. Constr. Mater.* **2026**, *25*, e06389. [CrossRef]
69. Wang, Y.; Zhang, N.; Zhang, S.; Wang, Y.; Xia, R.; Zhang, Y. A novel self-cleaning ceramic waste-slag geopolymer with nano-SiO_2-TiO_2 photocatalytic coating. *Ceram. Int.* **2024**, *50*, 17135–17144. [CrossRef]
70. Yang, Y.; Liu, C.; Zhang, S.; Li, B.; Ji, T. Photocatalytic NO_x removal and self-cleaning performance of polymeric carbon nitride functionalized alkali-activated slag composites. *J. Environ. Chem. Eng.* **2024**, *12*, 113675. [CrossRef]
71. Fansuri, H.; Alief, M.N.; Nurlina, N.; Nurherdiana, S.D.; Al Bakri Abdullah, M.M.; Subaer, S.; Ediati, R.; Lestari, W.W.; Mukti, R.R.; Utomo, W.P.; et al. Photocatalytic geopolymer membranes from Indonesian fly ash: TiO_2 integration, stability, and methylene blue degradation. *Case Stud. Chem. Environ. Eng.* **2025**, *12*, 101292. [CrossRef]
72. Li, H.; Zheng, Y.; Gong, G.; Su, X.; Shao, A. Simultaneous mechanical reinforcement and photocatalytic activation in UHTCC: Dual-function design via C and N co-modified TiO_2. *Constr. Build. Mater.* **2025**, *492*, 142846. [CrossRef]
73. Liao, G.; Yao, W.; She, A. Enhanced self-cleaning capacity of RBP@TiO_2 based building coating: Synergetic effect of photocatalysis and photo-induced superhydrophilicity. *Constr. Build. Mater.* **2023**, *388*, 131699. [CrossRef]
74. Liao, G.; Yao, W.; She, A.; Shi, C.; Zuo, J.; Wu, D. Interfacial design of nano-TiO_2 modified recycled concrete powder for building self-cleaning. *Colloids Surf. A Physicochem. Eng. Asp.* **2023**, *661*, 130925. [CrossRef]
75. Marconi, E.; Visone, F.; Graziani, V.; De Carlo, A.; Ismail, N.; Tortora, L. Polyhydroxyalkanoate/TiO_2 nanocomposite as sustainable coating for protection of marble, basalt, and travertine in the conservation of cultural heritage assets. *J. Cult. Herit.* **2026**, *80*, 102–109. [CrossRef]
76. Chobba, M.B.; Weththimuni, M.L.; Messaoud, M.; Urzi, C.; Bouaziz, J.; De Leo, F.; Licchelli, M. Ag-TiO_2/PDMS nanocomposite protective coatings: Synthesis, characterization, and use as a self-cleaning and antimicrobial agent. *Prog. Org. Coat.* **2021**, *158*, 106342. [CrossRef]
77. Yaghoubi, H.; Taghavinia, N.; Alamdari, E.K. Self cleaning TiO_2 coating on polycarbonate: Surface treatment, photocatalytic and nanomechanical properties. *Surf. Coat. Technol.* **2010**, *204*, 1562–1568. [CrossRef]
78. Zhou, J.; Tan, Z.; Liu, Z.; Jing, M.; Liu, W.; Fu, W. Preparation of transparent fluorocarbon/TiO_2-SiO_2 composite coating with improved self-cleaning performance and anti-aging property. *Appl. Surf. Sci.* **2017**, *396*, 161–168. [CrossRef]
79. Hooshyar, P.; Nafez, A.; Moghadasi, H.; Moosavi, S.A.; Moosavi, A. Experimental investigation of robust and hydrophobic solar cell cover glass with transparent, self-cleaning hybrid SiO_2/TiO_2 coatings. *Int. J. Thermofluids* **2025**, *29*, 101390. [CrossRef]
80. Kaveh, R.; Alizadeh, Z. Fabrication and characterization of a transparent, hydrophilic, and self-cleaning polyurethane coating on glass with a silica buffer layer and Ag_3PO_4/TiO_2 nanocomposite. *Prog. Org. Coat.* **2025**, *207*, 109382. [CrossRef]
81. Suwandecha, W.; Jiraborvornpongsa, N.; Sujaridworakun, P. Microwave-assisted facile synthesis of hollow MgF_2 nanoparticles for enhancing the optical properties of self-cleaning TiO_2 coatings. *Heliyon* **2025**, *11*, e44027. [CrossRef]
82. Xu, F.; Wang, T.; Chen, H.; Bohling, J.; Maurice, A.M.; Wu, L.; Zhou, S. Preparation of photocatalytic TiO_2 -based self-cleaning coatings for painted surface without interlayer. *Prog. Org. Coat.* **2017**, *113*, 15–24. [CrossRef]
83. Parasuraman, V.; Sekar, P.P.; Lee, H.; Sheraz, M.; Ly, H.N.; Bin Azizar, G.A.; Hong, J.W.; Lee, W.R.; Kim, S. Photocatalytic self-cleaning eco-friendly paint: A unique approach for efficient indoor air pollutant removal and surface disinfection. *Constr. Build. Mater.* **2024**, *412*, 134671. [CrossRef]
84. Jafarpisheh, F.; Kolvir, H.R.; Ghorbanpour, M. Photocatalytic self-cleaning and antibacterial activity of modified wood by Ag doped TiO_2 nanoparticles. *Next Mater.* **2024**, *4*, 100207. [CrossRef]
85. Wu, H.; Lu, X.; Feng, Z.; He, R. Dynamic hydrophobicity and surface reconstruction mechanism of self-cleaning traffic marking coatings incorporating modified TiO_2 nanoparticles. *Constr. Build. Mater.* **2025**, *497*, 143876. [CrossRef]
86. Zhang, F.; Guo, J.; Su, J.; Han, J. Empowering architectural glass fiber textiles with radiative cooling and photocatalytic self-cleaning performance through hybridization and morphology modulation of TiO_2 with diverse features. *Energy Build.* **2025**, *345*, 116110. [CrossRef]
87. Samuel, O.; Ullah Khan, A.; Kamaludin, R.; Othman, M.H.D.; Agustiono Kurniawan, T.; Imtiaz, A.; Faleh Al-Ogaili, M.; Usman, J.; Salisu Muhammad, M.; Abdulkareem, B.; et al. Dual layer hollow fiber photocatalytic membrane based on TiO_2-WO_3@GO composite with catalytic memory and enhanced anti-fouling and self-cleaning properties for oilfield-produced water treatment. *Chem. Eng. J.* **2024**, *483*, 149220. [CrossRef]
88. Smith, Y.R.; Subramanian, V. Heterostructural Composites of TiO_2 MeshTiO_2 Nanoparticles Photosensitized with CdS: A New Flexible Photoanode for Solar Cells. *J. Phys. Chem. C* **2011**, *115*, 8376–8385. [CrossRef]

89. Wang, P.; Wang, Y.; Zhang, P.; Chen, R.; Pang, B.; Kaur, R. Engineering multifunctional PMHS/TBT-DE-TiO_2 based superhydrophobic smart coatings: Application towards photocatalytic degradation of volatile organic compounds and building protection. *J. Build. Eng.* **2026**, *119*, 115146. [CrossRef]
90. Sheraz, M.; Ly, H.N.; Thi Le, V.C.; Nguyen, V.Q.; Naqvi, F.H.; Park, J.Y.; Lee, H.; Kim, S.; Lee, W.R.; Parasuraman, V. Electrospinning synthesis of CuBTC/TiO_2/PS composite nanofiber on HEPA filter with self-cleaning property for indoor air purification. *Process Saf. Environ. Prot.* **2023**, *172*, 621–631. [CrossRef]
91. Porcu, S.; Hazra, M.; Lodo, R.; Chiriu, D.; Ricci, P.C. Phenyl carbon nitride-based self-cleaning coatings: A sustainable solution for indoor air quality management. *J. Hazard. Mater. Adv.* **2026**, *23*, 101389. [CrossRef]
92. Jalvo, B.; Faraldos, M.; Bahamonde, A.; Rosal, R. Antimicrobial and antibiofilm efficacy of self-cleaning surfaces functionalized by TiO_2 photocatalytic nanoparticles against Staphylococcus aureus and Pseudomonas putida. *J. Hazard. Mater.* **2017**, *340*, 160–170. [CrossRef]
93. Zeng, Y.; Yang, X.; Peng, L.; Tian, Z.; Zou, Z.; Tang, A. Study of the self-cleaning performance of cement-based composites under different illumination conditions: Impact of nano-TiO_2 hydrogel modified with KH-570. *J. Build. Eng.* **2025**, *114*, 114263. [CrossRef]
94. Mekprasart, W.; Songpanit, M.; Sanyen, T.; Samart, S.; Chutipaijit, S.; Pecharapa, W.; Boonyarattanakalin, K. X-ray characterization, structural analysis, antibacterial activity, and self-cleaning property of Cu-doped TiO_2-SiO_2 nanocomposite prepared by sonochemical process. *Radiat. Phys. Chem.* **2024**, *225*, 112147. [CrossRef]
95. *BS EN 1096-5:2016*; Glass in Building—Coated Glass—Part 5: Test Method and Classification for the Self-Cleaning Performances of Coated Glass Surfaces. British Standards Institution: London, UK, 2016.
96. *ISO 22197-1:2016*; Fine Ceramics (Advanced Ceramics, Advanced Technical Ceramics)—Test Method for Air-Purification Performance of Semiconducting Photocatalytic Materials—Part 1: Removal of Nitric Oxide. International Organization for Standardization: Geneva, Switzerland, 2016.

Disclaimer/Publisher's Note: The statements, opinions and data contained in all publications are solely those of the individual author(s) and contributor(s) and not of MDPI and/or the editor(s). MDPI and/or the editor(s) disclaim responsibility for any injury to people or property resulting from any ideas, methods, instructions or products referred to in the content.